Abstracts in this section pertain to papers as Works-in-Progress at the 36th Annual Meeting of the SNM, June 13-16, 1989 held at the Alfonso J. Cervantes Convention Center, St. Louis, MO. Scientific Program Chairman: Peter T. Kirchner, MD

Bone/Joint

Posterboard 1120

CLINICAL APPLICATION OF Tc-99m LABELED GRANULOCYTES ANTIBODY IN BONE AND JOINT DISEASES.
A.Kroiss, F.Böck, G.Perneczky, Ch.Auinger, G.Weidlich, G.Kleinpeter, A.Neumayr. Institute of Nuclear Medicine, 1st Medical Department, Neurosurgical Department, Ludwig Boltzmann Forschungsstelle für klin. Geriatrie, KA Rudolfstiftung, Vienna, Austria, Europe.

The aim of this study was to proof the clinical relevance of monoclonal granulocytes antibody in combination with bone scintigaphy with Tc99m-diphosphonat in different bone and joint diseases.The immunoscintigraphy (IS) was perperformed with Tc-99m labeled antibody (BW 250/183; Behringwerke, FRG). The detections were done 4-6 and 24 hrs planar and in patients with diseases of the hip and spine SPECT pictures were performed too.

In 45 pts we performed the bone scintigraphy and IS, 25 male and 20 female, age from 18 to 81 yrs. In 7 pts we found an osteomyelitis, in 5 pts a coxitis and coxarthrosis, in 19 pts we could differentiate between septic loosening of hip prosthesis or a nonseptic, in 4 pts we found a septic process of the spine and in 4 pts a discitis. With this investigation we got good informations in pts after neurosurgical spine operations and fever and pain attacks (n=6). We found a sensitivity of 90% and a specificity of 86%.

In conclusion, the method is helpful for localization and extend of a septic process in bone and joint diseases.

Cardiovascular—Basic

Posterboard 1121

POSSIBLE MODELS FOR 11-C-ACETATE AS A TRACER FOR MYOCARDIAL METABOLISM.
A.Buck, G.Westera, M.J. van Eenige*, F.C. Visser*, GK. von Schulthess. University Hospital ,Nuclear Medicine, Zürich, Switzerland and * Free University Hospital, Cardiology, Amsterdam, The Netherlands

The feasibility of a model for the acetate kinetics in the heart has been studied.

On the basis of biochemical considerations a three compartment model, describing two parallel (A and B) pathways for metabolism and clearance, with the first compartment shared by both pathways was considered (Scheme).

Assuming for the input curve a linear increase over the first 30 sec, followed by an exponential decrease wth T1/2=30 sec the time activity (T-act) curve was calculated from the differential equations for various values of K1-K5 by numerical methods.

Assuming 10% increase in the individual k-values, we calculated the effect on the resulting T-act curves. We also calculated the sum of squares for 13 points on the curves, in dependence on the percentage increase of the individual k values.

If pathway B was small compared to A, only variations in K1, K2 and K3 caused variations in the shape of the T-act curve. The reverse of this argument implies, that from such T-act curves at best only these k's can be determined.

If for the clearance of 11-C activity only one major metabolic product (CO_2) is found, combined with a biexponential curve, this implies restriction to pathway A with similar values for K2 and K3.

If two major products are found, this implies both pathways. This leads to a monoexponential washout (like found by some investigators) if both pathways proceed at the same rate and either K2 + K4 (metabolism) or K3 + K5 (passage over the cell membrane) are rate determining.

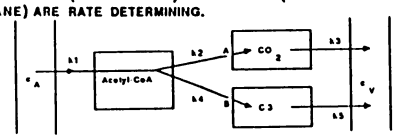

Posterboard 1122

DETECTION OF ACUTE CARDIAC INJURY WITH TECHNETIUM-99M GLUCARIC ACID.
B. Fornet, T. Yasuda, R. Wilkinson, M. Ahmad, R. Moore, B.A. Khaw, A.J. Fischman, H.W. Strauss. Massachusetts General Hospital, Boston, MA.

Glucaric acid, a 6 carbon dicarboxylic acid, forms a stable complex with Tc-99m following stannous reduction of pertechnetate. Normal tissue concentrates minimal amounts of this radiopharmaceutical, but areas of acute ischemic injury have markedly increased uptake of Tc-99m glucaric acid (Tc-Glu). This study was performed to compare the relative uptake of Tc-Glu to Indium-111 antimyosin antibody (In-AM) in rats with acute coronary occlusion. Two groups of animals were studied: A. Controls had thoracotomy only, without coronary ligation (n=8); and B. Coronary ligation. In-AM and Tc-Glu were administered 1 & 4 hours after ligation respectively. The animals were killed 1 hour after Tc-Glu administration, the heart was sliced into 1 mm thick breadloaf pieces and dual tracer autoradiographs were recorded. The average zone of uptake was 54 mm^2 with Tc-Glu and 34 mm^2 with In-AM ($p<0.0001$).

These data suggest that Tc-Glu identifies the zone of injury and necrosis. Further comparison is necessary to determine if Tc-Glu behaves like deoxyglucose.

Posterboard 1123

MONITORING THROMBOLYSIS WITH A Tc-99m MONOCLONAL ANTIBODY REACTING WITH PLATELETS: RESULTS OF IN VITRO STUDIES.
G-J Wang, Z.H. Oster, P. Som, and P.O. Zamora. SUNY Stony Brook School of Medicine, Brookhaven National Laboratory, Upton, NY. and Summa Medical Corporation, Albuquerque, NM.

We reported previously that Tc-99m-50H.19, a monoclonal antibody reacting with platelets can be used for imaging intravascular thrombi. The goal of this study is twofold: to investigate possible effects of aspirin (As) and heparin (Hep) on binding of Tc-99m-50H.19 to clot and to determine whether Tc-99m-50H.19 can be used for monitoring thrombolysis.

Human and dog clots were incubated with Tc-99m-50H.19 to maximum binding time. The radiolabeled clots were then incubated with As or Hep for 20 hr. After washing the clots, Tc-99m activity and dry weight were measured. Some clots were pre-incubated with As and Hep for 20 hr prior to Tc-99m-50H.19 addition, and Tc-99m activity and dry weight were measured. Serial dilutions of streptokinase (SK), or urokinase (UK) were added to clot and dry weight and residual activity were again determined. The effect of pre-incubation with As, Hep and the thrombolytic agents on the stability of Tc-99m-50H.19 antibody preparation was determined by thin-layer-chromatography.

As, Hep, SK and UK did not remove the Tc-99m label from the antibody. No effects on antibody binding to clot due to As or Hep were found. The decrease in clot weight incubated with SK and UK was proportional to the decrease in Tc-99m activity in clots.

It seems, therefore, that As or Hep will not cause false negative imaging results. These preliminary results indicate that Tc-99m-50H.19 is a promising agent for monitoring thrombolysis

Cardiovascular—Clinical

Posterboard 1124

MEASUREMENT OF REGIONAL MYOCARDIAL PERFUSION USING TC-99M TEBOROXIME (CARDIOTEC®†) AND DYNAMIC SPECT. W.E.Drane, M. Decker, P.Strickland, A.Tineo, S. Zmuda. University of Florida School of Medicine, Gainesville, FL.

Tc-99m teboroxime is a new myocardial perfusion agent that displays unique imaging characteristics (high myocardial extraction and rapid washout). Its washout kinetics support the use of rapid SPECT acquisitions. Since washout is a reflection of blood flow, it may prove useful for measurement of regional myocardial washout rates as an indicator of coronary artery disease (CAD). We studied 15 individuals (10 patients suspected of CAD, 5 normal volunteers) with dynamic SPECT using a multi-headed SPECT camera (TRIAD®*). Using separate stress and rest injections of Tc-99m teboroxime, each patient had serial 2 minute SPECT scans for 20 minutes. Interpretation was performed using initial 2 min stress scan vs. initial 2 min rest scan and each dynamic series was quantitated as to regional washout rate. The inital scans were compared to normalized scans at 18 - 20 min to observe for evidence of "redistribution". Imaging results were compared to coronary arteriography in the 10 patients and to stress thallium exams in the 5 volunteers.

Tc-99mTeboroxime SPECT was abnormal in 9 of 9 patients (100%) with significant CAD (stenosis > 50%). Four of 6 "normals" had normal scans (preliminary specificity = 67%). Analysis of regional washout rates in the 2 normals with false-positive scans appear to prevent their misdiagnosis. There was a moderate indirect correlation between regional washout at 20 minutes and percentage stenosis on arteriography ($r = -0.56$, $p < .0001$).

Tc-99m teboroxime dynamic SPECT using the TRIAD allows very short imaging times (≈ 2 min) [& potential rapid throughput] for stress/rest imagin; in the evaluation of ischemic heart disease. Analysis of regional washout also appears to detect significant coronary artery disease without the need for the separate stress/rest scans. Quantitation of regional washout with dynamic SPECT is possible and shows potential for the diagnosis of CAD. Further work is needed to substantiate its validity in this role, particularly in regard to specificity.

†Squibb Diagnostics, Inc., Princeton, NJ
*Trionix Research Laboratory, Inc., Twinsburg, Ohio

Posterboard 1125

EVALUATION OF RADIONUCLIDE BLOOD POOL VENOGRAPHY FOR THE DIAGNOSIS OF DEEP VENOUS THROMBOSIS. R.J. Gorten. Kelsey-Seybold Clinic, Houston, TX.

Radionuclide blood pool venography (BVP) has recently been developed and heralded as a screening test with advantages over previous methods. To assess the accuracy and usefulness in actual clinical problems, BPV and radionuclide flow venograms (FV) were performed within 3 days of each other on 40 patients referred for leg pain or swelling of uncertain etiology.

Interpretations were recorded for each method without knowledge of the other or clinical information. Final diagnoses, treatments, and responses were later obtained from chart reviews without knowing test results.

BPV and FV were in agreement for sites of abnormalities or absence thereof in 26/40 (65%) patients and in this subgroup, interpretations were substantiated in 91% in whom follow-up information was available. When the 2 methods were not in agreement, BPV was slightly more often correct. In the entire group, BPV was correct in 24/26 (92%) and FV in 22/26 (85%) when abnormalities below knee level only were excluded. When all sites were considered, BPV was accurate in 28/35 (80%) and FV in 26/35 (74%). In 5 patients, the chart follow-up information was not adequate for determination of probable final diagnosis.

In conclusion, BPV is more accurate, faster, simpler, and less discomforting than FV in actual clinical use.

Posterboard 1126

SPECTRAL ATTENUATION CIPHERS: A METHOD FOR ATTENUATION CORRECTION - THE Tl-201 PARADIGM. R.S. Hattner, A.S. La Pidus, J.W. O'Connell, L. Kaufman, H.D. Levin, D.A. Ortendahl, and E.H. Botvinick. University of California, San Francisco

Attenuation is a problem in scintigraphy - especially with Tl-201. Useful attenuation correction should permit quantitation and mitigate artifacts from uneven tissue absorption. Methods proposed for attenuation correction for SPECT are suboptimal. Here is a method, based on differential attenuation of unlike energies in a nuclides spectrum.

Ten % of Tl-201 decays result in a 167 KeV photon and 94% in 75 KeV Hg-201 x-rays. The detected ratio of these photons should vary with the thickness of interposed absorber. This effect was sought using Tl-201 and varying absorber thicknesses, and a scintillation camera. Effects of scatter from the 167 KeV photon into the Hg x-ray window were tested with p,5n I-123, a mostly unique source of similarly energetic photons, 159 KeV. The detected ratios precisely code attenuation path length over a useful range of absorber thickness, and scatter can be ignored. For I-123 scatter to photopeak ratios also appear to code depth. This may permit the application of this strategy to nuclides with simple spectra like Tc-99m. Clinical implementation is in progress and looks promising.

Posterboard 1127

LEFT VENTRICULAR FUNCTION AT ANAEROBIC THRESHOLD AND PEAK EXERCISE. F.H.Hironaka, M. Wayngarten, C.E.Negrão, M.U. Brandão, C.Giorgi, J.C.Meneguetti, E. Rondon, A.Santomauro, G.Bellotti, L. G.Serro Azul, F. Pileggi, E.E.Camargo.- The Heart Institute, São Paulo, Brazil.

Radionuclide derived parameters of left ventricular function during exercise of normal male subjects were studied simultaneously with pulmonary gas exchange analysis to provide better understanding of influence of age. 12 subjects (group A) aged 30 ± 4 yr and 16 older subjects (group B) aged 73 ± 3 yr were submitted to bycicle ergometer, at semi-recumbent position.

Ejection Fraction (EF), Peak Filling Rate (PFR) Peak Ejection Rate (PER), calculated from gated equilibrium study, and oxygen uptake(VO_2), measured directly, were analysed: 1) at rest(R) 2) at Anaerobic Threshold (AT) and 3) at Peak Exercise (PE).

State	R		AT		PE	
group	A	B	A	B	A	B
EF	63 ± 6	63 ± 5	75 ± 5	70 ± 5*	78 ± 5	70 ± 5*
PFR	$2.4\pm.3$	$1.8\pm.3$*	$5.1\pm.7$	$4.2\pm.7$*	7.4 ± 1.1	$5.2\pm.7$*
PER	$3.1\pm.6$	$2.5\pm.4$*	5.2 ± 1.3	$3.6\pm.5$*	6.7 ± 1.6	$4.0\pm.6$*
VO_2	$4.0\pm1.$	$3.6\pm.7$	16.6 ± 3.5	19.5 ± 5.8	26.2 ± 5.2	26.3 ± 4.2

*$p < 0.05$ vs group A

Submitted to similar cardiovascular loads, measured by oxygen consumptions, systolic derived parameters are more depressed at exercise in older group.

Posterboard 1128

^{201}Tl SINGLE PHOTON EMISSION COMPUTER TOMOGRAPHY (SPECT) AFTER ADENOSINE-INFUSION IN PATIENTS WITH ISCHEMIC HEART DISEASE (IHD). A Nolegren, D Bone, A Edlund, L Grip, P Henriksson, B Svane and A Ovall. Department of Clinical Physiology, Thoracic Clinics, Karolinska Hospital, S-104 01, Stockholm, Sweden.

We wanted to explore the possibility of using the natural vasodilator adenosine as an alternative to dipyridamol for provoking myocardial ischemia in patients with IHD.

Seven patients (5 male) with a mean age 62 years (range 53-68) accepted for bypass surgery were included in the study. There were 5 smokers. Six patients had previous myocardial infarctions. Four patients had a history of severe angina pectoris.

Coronary angiography was performed in all patients. Patients underwent symptom limited exercise myocardial ^{201}Tl SPECT and within one week ^{201}Tl SPECT after infusion of stepwise increases of adenosine concentrations. Endpoint for exercise administration of ^{201}Tl was angina pectoris in one, breathlessness in three and leg fatigue in four and for ^{201}Tl administration during adenosine infusion a dose of 107 μg/kg/min (70-120 μg/kg/min). Tomography was performed 10 min and 3 hours following ^{201}Tl injection in both studies. Results were compared by polar presentation of the left ventricular myocardium was used.

The mean activity administered was 94 MBq (86-98 MBq) during exercise and 93 MBq (90-96 MBq). Visual examination of the scintigrams by two investigators showed very good agreement.

There were no significant differences between the count distribution in the polar tomograms or in the observed perfusion defects. Redistribution after 3 hours was identical.

In conclusion adenosine infusion offers a powerful alternative to exercise and dipyridamol provocation in connection with ^{201}Tl myocardial SPECT in patients with ischemic heart disease.

Posterboard 1129

EXERCISE RADIONUCLIDE VENTRICULOGRAPHY AS A PREDICTOR OF CARDIAC EVENTS IN CORONARY INSUFFICIENCY. J.N Talbot, S. Witchitz, P. Toussaint, A. Boubaker, B. Mensch. Hôpital TENON, F 75020 PARIS, FRANCE.

The prognostic value of exercise Tc-RBC ventriculography (RNV) was prospectively studied in 59 pts with coronary insufficiency (CI) and positive cyclo-ergometric testing, under medical treatment. The left ventricular ejection fraction at rest (EFr), occurrence of angina, ST segment depression and ejection fraction during submaximal exercise (EFe) were studied. D = EFe - EFr was calculated.

All pts were followed for 6 to 36 months. No cardiac event occurred in 40 pts: group I; follow-up 21±11 months. In group II (19 pts; follow-up 16±13 months), there were 3 cardiac deaths, 1 myocardial infarction, 4 heart failures, 11 myocardial revascularizations (9 CABG, 2 PTCA).

A significant difference occurred between the 2 groups only for EFe, EFr and D. An index "I", composed of EFe and D, was determined by multivariate analysis to separate the 2 groups.

Results :	Grp I	Grp II	Chosen cut-off	Sensi tivity	Specif icity
EFr	59±12%	46±17%	50%	0.53	0.80
EFe	61±11%	41±17%	50%	0.74	0.90
D	+2.5±8%	-5±9%	-5%	0.53	0.88
I	0.2±0.2	0.6±0.3	0.3	0.79	1.00

In conclusion, exercise RNV has a predictive value in pts treated for CI; I and EFe are more discriminating than the formerly proposed D.

Posterboard 1130

MULTICENTER CLINICAL TRIAL OF 99M-TC TEBOROXIME (SQ30,217; CARDIOTEC) AS A MYOCARDIAL PERFUSION AGENT. J.S. Zielonka, Squibb Diagnostics, Princeton, NJ; R. Bellinger, David Grant Hospital, Travis AFB, CA; R.E. Coleman, Duke U., Durham NC; W. Drane and C. Williams, Shands and Gainesville VA Hospitals, Gainesville, FL; M. Goris, Stanford U. Hospital, Stanford, CA; L. Johnson and D. Seldin, Columbia Presbyterian, NYC, NY; J. Leppo, U. Mass., Worcester, MA; R. Reba and A. Wasserman, George Washington U. Hospital, Washington, DC.

A total of 194 subjects were studied with the test drug during Phase II/III clinical trials conducted at eight investigational centers.

Subjects were studied during rest (RE) and stress (ST) states. Exercise was conducted until the heart rate reached at least 85% of the predicted maximum or until symptoms precluded further exercise. Each subject was injected with 12-40 mCi of 99m Tc-teboroxime (TBO) followed by image acquisition. Moderate exercise was continued for approximately 90 seconds after the ST study injection. RE studies followed 1.5-2.5 hours later in order to ensure that the subjects were in true "rest" condition. Where the RE study preceded the ST study, ST studies were initiated in less than one hour after the RE test had been completed.

177/194 subject studies were categorized as evaluable for efficacy. All 194 subjects were included in safety analysis statistics. Investigators rated image quality as Fair or Good in 92% of the studies and poor in 8%. Rapid clearance of blood and lung fields permitted data acquisition to begin as soon as 90 seconds post injection.

The sensitivity and specificity of TBO imaging in 177 subjects were 84.1% and 91.0% respectively based on combined blinded and unblinded readings. Sensitivity and specificity values for Tl-201 based upon combined blinded and unblinded readings have been reported to be 82% and 91% respectively by Okada et. al., and 89% and 93% respectively for Massi et. al.

TBO imaging agreed with Tl-201 in 90.9% of the cases. Coronary angiography agreed with TBO and Tl-201 in 75.4% and 80.3% of the cases respectively. TBO appears to correlate more favorably with Tl-201 than with coronary angiography. However, this is not surprising, since both Tl-201 and TBO are both perfusion agents, while coronary angiography provides information on morphology (larger vessels).

TBO was found to be effective as a myocardial imaging agent. The myocardial kinetics of the drug, makes possible a stress and rest procedure to be performed in approximately one hour when the rest study precedes the stress study, or within 2-3 hours when the stress study is performed first. Clinical experience has demonstrated rapid, high myocardial uptake of TBO consistent with these reported findings. No redistribution of tracer was observed by any of the investigators throughout the trial.

Computers and Data Analysis

Posterboard 1131

KIDNEY DEPTH FROM RADIONUCLIDE RENAL STUDIES E. Byrom Michael Reese Hospital, Chicago IL

An estimate of kidney depth for attenuation correction is needed to measure function in dynamic radionuclide renal studies. To measure the depth by a radionuclide method, patients are imaged supine: after injection of Tc-99m-DTPA, posterior dynamic computer images are obtained for 25 minutes, followed by right (r) and left (l) lateral static images. On the computer display, the operator marks the center of the kidney in the lateral view. A program searches activity profiles for the maximum second derivative, constructs a continuous edge (the patient's back) by a least cost method, and reports the distance from kidney to back. To evaluate the technique, measured depths were regressed against weight/height ratio (w/h) for a group of 41 patients (all non-pediatric cases with two functioning kidneys studied in a 3 month period). The regression slopes of 12.30±2.30 (l) and 13.00±3.09 (r), agree with the usual formula, 13.3w/h + 0.7. The intercepts, 3.88±1.08 (l) and 3.79±1.45 (r), are larger, since depth is measured to the center rather than the surface of the kidney. Mean depths were 9.51cm (l) and 9.74cm (r): paired differences were not significant (p=.106). Individual depth differences of up to 3cm were noted, both from the contralateral kidney and from the regression line. In conclusion, measurement is necessary, since individual kidney depths may differ from the w/h estimate. This method provides a measured value as part of the radionuclide study and agrees with accepted average values.

Posterboard 1132

CORRECTION OF SPATIAL DISTORTIONS IN MR AND PET IMAGES FOR STRUCTURE-FUNCTION REGISTRATION. P.D. Cutler, S. Sinha, M. Dahlbom, and E.J. Hoffman. UCLA School of Medicine, Los Angeles, CA.

In order to accurately register intra-subject images from PET and MRI modalities, the type and severity of spatial distortions which occur in these images were characterized. Effects of these distortions on the registration process were also measured.

Lucite phantoms were designed and fabricated to measure planar and axial distortions in both scanners. Fillable holes in the phantom appear as small dots whose centroids are used to determine planar or axial mispositioning in each region of the imaged volume. The following imaging protocols were used: 45 PET planes at 2.25 mm axial spacing on a CTI/831 neuro-PET system; 30 MRI planes at 4.2 mm axial spacing on a FONAR B-3000 resisitive MRI system using a T1-weighted spin-echo sequence.

Distortions in the ECAT were found to be small (~1 mm at the edge of the field of view) and limited to planar mispositioning due to inherent non-linear sampling in circular PET systems. These distortions are well-characterized and easily corrected. MRI distortions were more severe and image-dependent. Axial skewing of as much as 8-10 mm occurs when transaxial planes are stacked. Tilting or warping of the image planes away from the true transaxial plane was slight, as was in-plane "pin-cushion" or "barrel" distorion. A protocol that uses multiple acquisitions stacked or interleaved results in additional alignment problems.

Compared with corrected image volumes, uncorrected data were found to cause misregistrations of 5-15 mm, due primarily to the axial skewing and multiple-acquisition misalignment.

Posterboard 1133

ATTENUATION CORRECTION OF THALLIUM SPECT USING DIFFERENTIAL ATTENUATION OF THALLIUM PHOTONS. C.L. Hansen, J.A. Siegel, W.A. Van Decker, and A. H. Maurer. Temple University Hospital, Philadelphia, PA.

Tl-201 SPECT is a commonly used technique for the detection of coronary artery disease. It is well known that scatter and photon attenuation greatly affect image quality and quantitation. These inherent SPECT problems are amplified by the low energy emissions of Tl-201. This study examined the feasibility of using the ratio of Tl counts from its upper 135 and 167 keV photopeaks (high) to its lower 69.8-80.3 keV peak (low) to correct for the effects of attenuation using a first-order SPECT post-processing correction. Initially, a planar study was performed to develop a regression equation that would correct for the attenuation of low energy counts as a function of the low/high count ratio. This was done using successive thicknesses of tissue-equivalent material for a thickness up to 20 cm. Next, four tubes of 1.2 cm diameter and 10 cm length were placed 3.5 cm apart. The tubes were filled with 100 uCi of Tl-201 each and first imaged in air and then in a water-filled cylindrical phantom. 180° SPECT studies were performed using dual-energy windows (20% for the high and 25% for the low) to acquire counts from the above three energy peaks. The low and high energy acquisitions were reconstructed separately. The low energy SPECT reconstructed slices were then corrected for attenuation on a voxel by voxel basis using the previously determined regression equation. Count profiles were drawn through the reconstructed tubes in air and in water both before and after attenuation correction. The peak counts of the tubes in air were constant. The peak counts for the uncorrected water slices varied from 37% to 17% of that in air and the corrected water slices varied from 83% to 75%. We conclude that attenuation correction for 180° Tl SPECT using both the high and low energy emissions may allow for more accurate image quantitation.

Posterboard 1134

EVALUATION OF A NEW QUANTITATIVE ALGORITHM FOR MYOCARDIAL PERFUSION TOMOGRAPHY. L. Mortelmans, J. Nuyts, P. Suetens, A. Oosterlinck, M. De Roo, K.U.Leuven, Leuven, Belgium.

A new delineation algorithm for cardiac Spect images using only radial slices through the long axis was developped. The myocardial boundaries are delineated by a minimum cost algorithm which uses gradient information and a model of left ventricular shape. The valve plane is determined by an iterative least square method. Data reduction is performed by constructing two polar maps ("Bullseyes") containing count rate and volume information.

Twenty-eight measurements of a Jasczack heart phantom, fixed in a cylinder, were performed with various target to background ratios. In addition a series of artificial SPECT images was analysed to evaluate the influence of the wall thickness on the volume calculations. A threshold of 40% was used for the delineation of the hypoactive region.

The delineation of the ventricle is rather constant and noise independent even in infarcted zones. Total volume was overestimated by 26% with a s.d. of 5%. Artificial images showed that overestimation is highly dependent on wall thickness. Measurements in air showed a good estimation of relative infarct size (error<10%). In water the relative error increases with decreasing infarct volume (25% and 12% for an infarct volume of 10% and 28% respectively).

This method of measuring relative infarct size produced reproducible data. The overestimation is probably due to partial volume effect. Correction for attenuation, scatter and resolution is under study.

Posterboard 1135

EFFECTS OF RECONSTRUCTION ALGORITHMS ON NON-STATIONARY SPECT IMAGE NOISE J.A.Terry, B.M.W.Tsui, D.R.Gilland. University of North Carolina, Chapel Hill, NC.

Efforts to study CT image noise usually include the calculation of average noise power spectra, a calculation which involves an assumption of stationary noise. However, CT noise is not stationary. We studied the non-stationary properties of SPECT imaging noise obtained from using the filtered-backprojection (FB) and maximum likelihood-expectation maximization (ML-EM) reconstruction algorithms. Autocovariance functions were determined for various regions (of size 10x10) at different locations within a reconstructed image (64x64); using 100 images, an ensemble average was calculated for each local autocovariance function. Test images were obtained from a simulated uniform disk phantom with Poisson noise added to the projection data, where the total counts in the projection is 565,000. For the FB algorithm with a Hamming filter, the variance decreases from the central to the most peripheral region by as much as 21.7 percent. However, the shape of the autocovariance function of the most peripheral region was slightly narrower (indicating a sharper noise) than that of the central region. For the ML-EM algorithm after 25 iterations, the variance increases from the central to the most peripheral region by as much as 15.0 percent. The shape of the autocovariance function of the central region was slightly narrower than that of the most peripheral region. Our investigation shows that the non-stationary noise characteristics of SPECT images depend on the reconstruction algorithm used.

Posterboard 1136

THREE-DIMENSIONAL VISUALIZATION OF HUMAN BRAIN STRUCTURE-FUNCTION RELATIONSHIPS. D.J. Valentino, P.D. Cutler, J.C. Mazziotta, H.K. Huang, †C.A. Pelizzari, †G.T.Y. Chen, E.J. Hoffman, M.E. Phelps.
UCLA Dept. of Radiology, Los Angeles, CA,
†University of Chicago, Dept. of Radiation Therapy, Chicago, IL.

This paper describes a new technique for visualizing the complementary structural and functional information in magnetic resonance imaging (MRI) and positron emission tomography (PET). MRI data was obtained on a FONAR B-3000 scanner using an inversion recovery sequence (TE=30 msec, TI=300 msec, TR=1276 msec, 4.0 mm x 30 slices). High-resolution 18-FDG PET images were obtained on a Siemens-CTI 831 scanner (5 million counts, 6.0 mm x 30 slices). These image volumes were correlated using a surface-fitting technique [1] and three-dimensionally visualized using a new approach to volume imaging.

New procedures were developed, using a volumetric imaging technique [2], to "texture-map" brain glucose metabolism onto brain anatomy. Sequences of three-dimensional views (3-D images) were produced and displayed dynamically to indicate the 3-D relationship between brain structure and brain function; these 3-D structure-function relationships are essential to our understanding of the normal and pathologic brain.

[1] Pelizzari CA, Chen GTY, et al (1989): J Comput Assist Tomogr, 13(1):20-26.
[2] Drebin, RA, Carpenter, L, Hanrahan P, (1988): Computer Graphics, 22(4):65-74.

Posterboard 1137

SCATTER AND BACKGROUND SUPPRESSION IN NUCLEAR MEDICINE IMAGING. J.P. Windham, Cathy Mast, Don Peck, Henry Ford Hospital, Detroit, MI.

In Nuclear Medicine Imaging, the major factors limiting contrast are the presence of background activity and scattered radiation. Information pertaining to these image degrading factors can be found in the energy spectrum of the radiation detected by the gamma camera. We have developed a specific linear filter which, when applied to a multi-spectral set of images of the same object, produces a single composite image in which a desired feature (process) is segmented and one or more undesired features (processes) are suppressed (1). In our implementation of the filter to the above contrast problem, a multiple-energy set of images is obtained allowing for a multi-spectral description of the imaging process. The primary radiation spectrum is taken as the desired process while the scatter and the background spectra are taken as undesired processes to determine the weighting functions to be used in the linear filter. In the filtered image, the primary radiation contribution is enhanced while those of the scatter and background components are suppressed. Initial findings indicate that the technique is independent of thickness of scatter medium and provides a contrast improvement of 50%. Applications to phantom studies will be presented.

1. J.P.Windham, et.al, "Eigenimage Filtering in MR Imaging",JCAT 12(1):1-9, 1/88.

Posterboard 1138

Quantitative Calculation of GFR using Tc-99m DTPA Camera Images

I.George Zubal, *Vicente Caride, Eileen O. Smith, Paul B. Hoffer

Department of Diagnostic Radiology, Section of Nuclear Medicine, Yale School of Medicine,
*Department of Radiology, Section of Nuclear Medicine St. Raphael's Hospital
New Haven, Connecticut

By using the quantitative measurements obtained from camera images of the kidneys and from patient physio-parameters, a direct calculation of GFR is shown to be feasible.

GFR values are calculated from the fraction of the injected dose, F, found in the kidneys using an estimation of the kidney depth. An additional estimate of the patient blood volume is derived from the ICRP No. 23 equation: $V = 95.7 \times W - 274$ (where W is the patient's weight in kilograms and V is the blood volume in cc). The plasma volume, P, is calculated from each patient's hematocrit,H, using the relation $P = V \times (1-H)$.

A quantitative GFR can be calculated for each patient, using: $GFR = (F \times P/T)$ cc/min. T is the time over which the image was acquired (approx. 3 mins.). A total of 30 patients were studied (15 in each of two institutions). Each patient's GFR was calculated using the described camera technique and by calculating Tc99mDTPA blood clearance from blood samples. The total correlation coefficient was $R = 0.87$.

Dosimetry/Radiobiology

Posterboard 1139

RADIATION DOSE TO THE BLADDER WALL FROM 2-[F-18]-FLUORO-2-DEOXY-D-GLUCOSE BASED ON A DYNAMIC BLADDER MODEL. M. T. Dowd, C. T. Chen, M. D. Cooper, M. J. Wendell. The University of Chicago, Chicago, IL.

Accurate determination of the radiation dose to the bladder wall from 2-[F-18]-fluoro-2-deoxy-D-glucose (18-FDG) is important because the bladder is the critical organ in 18-FDG PET scans. The radiation dose to the bladder wall from injected 18-FDG was estimated using a dynamic bladder model, developed previously at this institution. This model takes into account excretion rate, the varying size of the bladder, the initial volume at the injection, and an assumed bladder time activity curve. The bladder uptake curve is a function with two exponential terms that is derived from the measured plasma 18-FDG curve. The excretion rate is assumed to be a constant, and is determined using the time of void before the injection, the time of void after the PET scan, and the volume of the post-scan void. This model is more accurate than the MIRD model, which assumes a constant bladder volume of 200 ml. The necessary parameters (time of void before injection, injection time, injected amount, time of void after injection, volume and radiation content of post-injection void) have been measured in over 500 subjects in a five year period. The current work is based on the 125 most recent of these subjects. Our data indicate that when the bladder is large at the time of injection, the dose to the bladder is greatly reduced. The dynamically calculated absorbed dose of the bladder for an initial volume of 100 ml is about .37 rad/mCi, while that for an initial volume of 400 ml is calculated to be .067 rad/mCi. The MIRD model would estimate a dose of .34 rad/mCi for both of these cases. Dose estimates also include the additional dose to the bladder wall after the first post-injection void. An evaluation of the calculated dose to the bladder wall for those subjects under 18 years of age as compared to those over 18 years of age has also been completed.

Posterboard 1140

DOSIMETRY OF I-125 SEED IMPLANTS USING SPECT. T. Lowinger, D.S. Marsden, A. Vallejo St. Luke's-Roosevelt Hospital New York, N.Y.

We have used SPECT to calculate the absorbed dose distribution for I-125 seed implants.

I-125 is widely used for permanent implants in radiotherapy. The dosimetry of I-125 is more complex than for conventional interstitial sources due to the structure of the seeds and emission spectrum. We have performed SPECT studies on both humans and phantoms. A Siemens orbiter scintillation camera interfaced to a computer was used to obtain 64 views in a circular orbit. A 99% window centered about 50 keV was used with a LEAP collimator. Absorbed dose distribution was evaluated two ways: 1.Localizing the seeds in space and, 2.Generating isocontour lines of activity distribution. Isodose curves were generated by integrating the dose rates over the source distribution. In the phantoms, seeds were localized within 8% of their true location in space and resulted in doses similar to radiographic localizations.

We conclude that SPECT can be useful in evaluating implant dosimetry and provide superior display of isodose curves and information in three dimensions.

Endocrine

Posterboard 1141

CONCURRENT BONE SCINTIGRAPHIC FINDINGS AND SERUM OSTEOCALCIN LEVELS. W.J. Shih, B. Wierzbinski, J. Collins, S. Magoun, J. Joyce , G. Conrad ,and UY Ryo. VA and Univ of Kentucky Medical Centers, Lexington, KY.

Osteocalcin is a non-collangenous bone protein produced by osteoblasts. Increase in serum osteocalcin level reflects osteoblast activity with acceleration of bone formation. To evaluate the correlation of Tc-HDP bone scintigraphic findings and concurrent serum osteocalcin, serum osteocalcin values of 40 consecutive patients were measured by radioimmunoassay at the time of initial referral for bone studies. These patients, all males, aged 23-93, were studied for various disease entities including prostate carcinoma. The results of the assay were categorized into 3 groups (gp) as follows: 17 at normal level (1.8 - 6.6 ng/ml) (gp 1), 21 low (gp 2) and 2 high (gp 3). Only 1 bronchogenic CA patient with a high level had a right iliac lesion suggesting metastasis. Nine patients' bone scans showed positive metastases with normal or low levels. Two patients with stress fractures as shown on bone scans had normal levels. Those patients with disparity between serum osteocalcin and positive bone lesions may be interpreted as follows: Instead of osteoblastic activity resulting in the synthesis and/or release of osteocalcin, area(s) of increased uptake in the bone scan may be predominantly reflecting increased regional blood flow and decreased sympathetic tone resulting in an increase in bone agent deposition.

Posterboard 1142

EFFECTS OF ANTI-THYROID MEDICATIONS ON THYROID SCAN IN PATIENTS WITH GRAVE'S DISEASE. E. Yeo, D. C. P. Chen, M. E. Siegel. LAC/USC Medical Center, Los Angeles, California

Anti-thyroid medications used in patients with Grave's disease can microscopically change the morphology of the thyroid gland. We studied the relationship between antithyroid medication and thyroid scan patterns in Grave's disease.

46 patients (14 male, 32 female) with Grave's disease were treated with antithyroid medications, i.e., propylthiouracil (PTU) or methimazole (MIM) for various duration prior to obtaining thyroid scan. 26 patients received PTU and 20 patients MIM. The duration of treatment varies from less than one month to more than 36 months. The thyroid scan and uptake were obtained with 200 uCi of I-123 capsule orally. The homogeneity of the scan was graded as 0= homogeneous, +1= inhomogeneous; +2= marked inhomogeneous.

All 23/26 patients treated with PTU or MIM for less than 11 months had homogeneous uptake in the thyroid gland, except 3 patients treated with PTU for < 11 months had inhomogeneous uptake. Among patients treated for > 12 months, 7/20(35%) had grade "o", 8/20(40%) had "+1", 9/20 (45%) had "+2" inhomogeneity. 5 out of 25 patients treated with PTU for 8 months to 3 years had 3+ inhomogeneity while none of 20 patients treated with MIM had 3+ inhomogeneity. 1 patient treated with PTU for 1 year had 3+ inhomogeneity and was surgically proven to have diffuse hyperplasia of the thyroid gland.

In conclusion, our preliminary findings raise the possibility that antithyroid medications may not only affect the microscopic morphology but the scan pattern also, in patients with Grave's disease and this may affect scan interpretation. A prospective study is underway to further determine the above.

Gastroenterology

Posterboard 1143

AGE RELATED REDUCTION IN NUTRIENT HEPATIC BLOOD FLOW. N. Milne, E.B. Rypins, J. Segal, I.J. Sarfeh, K.P. Lyons. VAMC Long Beach and U.C. Irvine, CA

Fasting volunteers with normal liver function (N=13) had dynamic hepatobiliary scintigraphy following iv bolus injection of 5mCi Tc-99m-Mebrofenin (TcMb). Serial 1 min images were acquired for 45 min after injection. Blood samples were drawn at 10 and 20 minutes and counted in a well-counter. Normalized time-activity curves were plotted from a region of interest over the cardiac blood pool. An exponential slope was fitted to the points between 10 and 20 min. Clearance in ml/min was obtained from the ratio between computer counts per pixel and counts per ml blood. Clearance = (dose X slope) / intercept and was normalized to body surface area ($1.73m^2$) Since TcMb first pass extraction is >95% and its extrahepatic elimination is <2%, TcMb clearance is equivalent to nutrient hepatic blood flow. Nutrient hepatic blood flow correlated inversely with age and fit the exponential: $Y = 2326*e^{-26.22X}$ ($r=.80$, $p=0.001$).

We conclude that, in man, nutrient hepatic blood flow diminishes with advancing age as has already been demonstrated in aging normal rats.

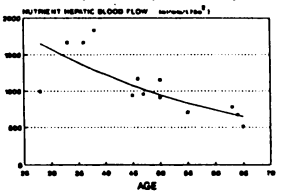

Posterboard 1144

REDUCED ACQUISITION TIME FOR SOLID PHASE GASTRIC EMPTYING. J.A. Siegel, J.L. Urbain, N.D. Charkes, and A.H. Maurer. Temple University Hospital, Philadelphia, PA.

The solid phase gastric emptying test is usually carried out for up to 2.5 hours. In an effort to perform the test in a more efficient fashion and to significantly reduce camera time, we examined the possibility of performing a 20 minute dynamic study at 90 postcibal minutes. Five normal volunteers underwent gastric scintigraphy using a dual-headed gamma camera after ingesting a meal consisting of a Tc-99m labeled egg sandwich and 300 ml of water. Images were acquired every minute for 150 minutes. Emptying curves were generated from both anterior only (ANT) and geometric mean (GM) data and then fitted to a power exponential function to enable the calculation of T1/2 and the lag phase (TLAG). The curves analyzed represented either data acquired at 15 minute intervals (q15), our normal technique, or an initial time zero image followed by a 20 minute dynamic study commencing at 90 postcibal minutes (dy). The results were as follows (mean ±1 SEM):

	GM		ANT	
	q15	dy	q15	dy
T1/2	95±12	95±12	108±16	108±14
TLAG	61±12	58±11	83±17	74±21

There were no significant differences ($p>0.05$) between the q15 or dy study for GM and ANT acquisitions for either T1/2 or TLAG. In addition, the differences between these two parameters were not significant between GM and ANT studies. We conclude that the clinical solid gastric emptying test may be performed by a 20 minute dynamic study, thereby, shortening the duration of the test and freeing up the camera for other studies.

Immunology/Infectious Disease

Posterboard 1145

CHARACTERIZATION OF HUMAN ANTI-MURINE ANTIBODY (HAMA) ACTIVITY IN THE SERA OF A SUB-POPULATION OF PATIENTS NOT INJECTED WITH MURINE MONOCLONAL ANTIBODY (MMAb). R.N. Duggal, H.J. Hansen, E.S. Newman and D.M. Goldenberg, Immunomedics, Inc, and Center for Molecular Medicine and Immunology, UMDNJ, Newark, NJ, 07103

"HAMA-like" activity has been reported to be present in the sera of patients with rheumatoid arthritis, RA (Cancer Res. 47:4520:4525, 1987). This study demonstrated that HAMA in these sera was primarily directed aganinst the Fc determinants of IgG; it was suggested that administration of intact MMAb may be contraindicated in these patients. Upon increasing the sensitity of the commercial ImmuSTRIP HAMA research assay (Immunomedics, Inc., Newark, NJ), by diluting sera 1/2 rather than 1/10 as recommended in the package insert, we have detected "HAMA-like" activity in the sera of many RA patients that have positive titers of rheumatoid factor (RF). However, the "HAMA-like" activity does not appear to be due to RF. HAMA titers of many of the RA sera are markedly reduced upon adsorption with a murine monoclonal antibody solid-phase (vinylidene fluoride), while RF titers are not reduced. Minimal reduction of "HAMA-like" activity was observed after adsorption of RF with heat-aggregated IgG, further confirming that the "HAMA-like" activity was not caused by RF. We are presently using the modified ImmuSTRIP HAMA assay to survey the sera of patients with other diseases that have elevated RF titers. This study has important relevance in the case of patients with known or occult infections, since RF is frequently elevated in these patients and many are candidates for imaging or therapy with MMAbs.

Posterboard 1146

THE CLINICAL SIGNIFICANCE OF PHOTOPENIA IN THE BONE ON INDIUM-111 LEUKOCYTE SCINTIGRAPHY. CP Gilles, MD Cerqueira, AF Jacobsen. University of Washington and Veterans Administration Hospital, Seattle WA.

Indium 111 scintigraphy has been utilized alone and as an adjunct to Tc-99m bone imaging in the diagnosis of osteomyelitis. While most Indium-labeled white blood cell scans show increased activity in infections of the bone, diminished or absent activity may be observed in regions of osteomyelitis.

During the past year, 11 patients suspected of having osteomyelitis or occult infection were found to have photopenic defects in the bone on WBC scanning. On concurrent bone scintigraphy, 8 of 11 patients had increased activity in the region of interest. The sites of skeletal involvement and number of cases were thoracic spine (4), lumbar spine (3), pelvis (3) and femur (1). The etiology of the cold defects were confirmed by radiography, myelography, computerized tomography, magnetic resonance imaging, or open biopsy for culture and histopathology. The photopenic defects were as a result of healed osteomyelitis (4), active osteomyelitis (3), metastatic disease (1), diskectomy (1) bone resection (1) and spondylolisthesis (1). Although photopenic defects in bone on WBC scanning most frequently reflect the effects of osteomyelitis, in our experience this finding does not distinguish active from healed infection.

Posterboard 1147

TECHNETIUM-99M LABELED NR-LU-10 MONOCLONAL ANTIBODY (MoAb) IN ASSESSING PATIENTS WITH SMALL CELL LUNG CANCER (SCLC). A. Sonin, B. McCook, D. Johnson, M. Sandler, J.Hainsworth, J. Clanton, J. Erland, R. Pfeffer, Vanderbilt, Nash.,TN. C. Faubion, P.Abrams, NeoRx,Seattle, WA.

Primary and metastatic disease in patients with SCLC is presently being investigated with Tc-99m NR-LU-10 (NeoRx) monoclonal antibody (MoAb). Preliminary data of 6 patients studied thus far is presented (see Table).

MoAb scan detected 34 of 36 total lesions found on plain films, CT, and bone scan. In addition, MoAb detected a total of 9 previously unsuspected metastatic lesions in two patients (#1 and #3).

Current preliminary data gives encouraging support to the utility of MoAb as a diagnostic modality to detect primary and metastatic disease in patients with SCLC.

	Conventional Modalities					MoAb		
Pt	Total # Lesions	XR	CT Body	CT Head	Bone Scan	#	% Detected	Previously Undetected
1	9	2	4	0	5	9	100	2
2	5	1	5	0	0	5	100	--
3	7	4	5	1	0	6[A]	86	7
4	1	1	1	0	0	1	100	--
5	8	2	4	1	3	7[B]	88	--
6	6	2	2	2	0	6	100	--

A = small pleural effusion not detected
B = 3 cm supraclavicular lymph node on physical exam, (not biopsied) not detected

Instrumentation

Posterboard 1148

PROTOTYPE TOTAL PERFORMANCE KINETIC KIDNEY PHANTOM, S.K. Chirala*, A.K. Basu, Deptt of Nuclear Medicine, All India Institute of Medical Sciences*, New Delhi and Bir Hospital, Kathmandu.

Though in common clinical use, the radionuclide renogram (RG) continues to be controversial. Reductionistic analysis of different variables in the synthesis of RG have not been informative. We have developed a prototype for a kidney phantom for quality assurance, standardisation and as an aid in teaching and research.

Prototype was developed with perspex compartments to represent different body compartments. Water served as plasma. Circulation was achieved by a peristaltic pump and tubes. I-131 Hippuran was injected into the tube leading to right ventricle compartment. The 'kidney' was monitored with a probe detector system and a 'renogram' was generated. The phantom RG had shown all the phases of RG as was originally described by Taplin et al.

The phantom renogram obtained validates model. The phantom can be used to understand the syntheses of renogram in different physiopathological conditions.

Posterboard 1149

REPRODUCIBILITY OF X-RAY BONE MINERAL DENSITY ANALYSER. S. Eberl, S. Johnson, M. G. Yeates, N. A. Pocock, J. A. Eisman, S. Ramsay. St. Vincent's Hospital, Sydney, Australia.

The aim of this study was to evaluate the reproducibility of the new dual energy X-ray Bone Mineral Analyser (DEXA) manufactured by Lunar Radiation Corp. and to compare it with a Gd-153 based unit (Lunar Radiation Corp. DP3).

The calibration phantom supplied with the instrument was scanned daily over a period of 10 months. A spine phantom constructed from human vertebrae was scanned weekly over a period of 6 months using both normal (DEXA Normal) and fast (DEXA Fast) scan modes on the DEXA instrument. In-vivo reproducibility was assessed by scanning 51 patients twice on the DEXA unit as well as once on the DP3.The two scans for each patient were all performed on the one day.

The following results were obtained for the phantom studies:

	Calibration	Spine Phantom	
	Phantom CV(%)	Mean BMD(g/cm²)	CV(%)
DEXA Normal	0.50 (n=200)	1.231 (n=49)	0.61
DEXA Fast	—	1.215 (n=30)	0.72
DP3	0.67 (n=204)	1.235 (n=39)	1.07

The following results were obtained for the patient studies:

	Lumbar Spine		Femoral Neck	
	r Value	SEE(g/cm²)	r Value	SEE(g/cm²)
DEXA Scan 1 vs 2	0.991	0.031	0.965	0.044
DEXA vs DP3	0.976	0.045	0.968	0.040

Reanalysis of all the DEXA scans by a single operator gave an SEE of .021 g/cm² for scan 1 vs 2. Good reproducibility of the DEXA unit was observed for the phantom studies. Correlation between the DEXA and the older DP3 unit for the patient studies was excellent. Reproducibility of the DEXA patient studies was better than that for the DP3 (previously measured at 0.05g/cm² SEE for the lumbar spine).

Posterboard 1150

A WHOLE BODY IMAGING TECHNIQUE FOR PET. T.M. Guerrero, E.J. Hoffman, M. Dahlbom, R. Hawkins, M.E. Phelps, UCLA School of Medicine, Los Angeles, CA.

An investigation of rapid whole-body PET scanning was performed with a view towards its eventual use in screening for metastatic lesions with F-18 labelled FDG or fluoride ion.

In contrast to the current rectilinear scan mode on the CTI 831 Neuro- and 931 Wholebody-PET systems, which collect only AP and Lateral views, the full set of tomographic data is collected for the full range of the scan. The sinogram data is resorted into whole-body projection images, which, when displayed in a cine mode, allow the observer to visually integrate and interpret the data in what is effectively a 3-dimensional format. In addition to developing the sorting routines, the effect of summing the projections over a number of angles and the effect of smoothing the data with a spatially variant smoothing kernel were also investigated. The amount of smoothing was varied inversely with the number of events per pixel averaged over 7 by 7 regions throughout the image.

Data were obtained on both PET systems following administration of 10 mCi of F-18 FDG, allowing 45 min for uptake. Each system simultaneously acquires 15 images at 6.75 mm intervals. Data were collected for 1, 2, and 4 min imaging periods per position with the patient bed being moved alternate 3.375 and 101.25 mm steps to provide a 3.375 mm z-axis sampling interval for the full length of the scan.

The images were of good quality for all scan intervals. Angular summing of up to 10.5 deg caused no apparent loss in resolution, while providing considerable improvement in image quality. With appropriate angular summing and/or spatial smoothing, good quality whole-body surveys of FDG distributions can be obtained in less than 30 minutes.

Posterboard 1151

DUAL ENERGY BRAIN SPECT - METHODS AND APPLICATIONS. S. Holm, L. Friberg, H.K. Iversen, N.A. Lassen. Dept. of Clinical Physiology and Nuclear Medicine, Bispebjerg Hospital, Copenhagen, Denmark.

A new fast rotating, 2-slice SPECT with 13 mm resolution (TOMOMATIC 232) has been studied with special regard to applications in research and clinical routine of its dual energy window facilities. Energy window settings are software controlled and each event analyzed by distributed micro-processors in the gantry before transmission to the MicroVaxII. Count losses are negligible at realistic count rates. The energy resolution (< 15% at 140 keV) is sufficient to separate, effectively, Xe-133 and Technetium-99m, as demonstrated in studies of a 2-compartment brain phantom. In addition to dual window scatter correction, the following applications are considered:

1) Simultaneous measurement of cerebral blood flow and volume (CBF and CBV). Following injection of 100 MBq Tc-99m labelled erythrocytes repeated Xe-133 inhalation studies are performed. On 6 normal volunteers the method has proven to be reproducible and respond adequately to changes induced by hyperventilation or by vasoactive drugs (acetazolamide, indomethacine). The method will be used in the study of migraine.

2) Correlative measurements of Tc/I-labelled flow-tracers and Xe-133 inhalation studies, eventually overcoming timing and positioning problems between measurements.

3) Improvement of attenuation correction from using simultaneous transmission/emission scans will be explored. An 8-slice whole-body SPECT based on the same principles is currently under construction.

Posterboard 1152

IMPROVED ACCURACY OF ATTENUATION CORRECTION IN WHOLE-BODY PET BY ADAPTIVE FILTERING OF TRANSMISSION PROFILES. H. Ostertag, W.K. Kübler, J. Doll, L.G. Strauss, W.J. Lorenz. Institut für Radiologie und Pathophysiologie, Deutsches Krebsforschungszentrum, Heidelberg, FRG.

The most serious problem in measured whole-body attenuation correction is due to insufficient counting statistics in the transmission scan profiles. These result not only in large statistical deviations but also in erroneous mean values for the attenuation correction factors. The magnitude of these errors, as a function of total image counts and of the counts in the transmission profiles, was studied with rectangular water phantoms. The attenuation lengths calculated from the measured attenuation data using $\mu = 0.096/cm$ were compared to the physical dimensions of the phantom. As an overall indicator of the accuracy of attenuation correction, the mean attenuation coefficient in the attenuation images was also determined. For a 35 cm x 24 cm phantom, 20 million counts are needed to reach a stable μ. By filtering the transmission profiles rather than the attenuation correction factors, a stable μ was reached already with 5 million counts. A simple count-dependent smoothing filter was used. The improved attenuation correction was tested by emission phantom measurements, and was then applied to patient studies.

Posterboard 1153

SIMULTANEOUS EMISSION AND TRANSMISSION SCANS IN PET USING A MASKED ORBITING TRANSMISSION SOURCE (MOTS).
C J Thompson N T Ranger* and A C Evans
McConnell Brain Imaging Centre, Montreal Neurological Institute and Medical Physics Unit
McGill University, Montreal, Canada

Transmission scans are performed using a point source of Ge-68 masked by lead into a fan beam of annihilation photons in each scanning plane of the tomograph. As the source orbits the patient section, detector pairs collinear with it accept data for the transmission scan. Coincident events between detector pairs nearly collinear with the source are rejected, while those far from collinear record an emission scan from activity in the patient slice. While this reduces the tomograph's emission event efficiency by 30% (7% transmission, 23% rejected), **slice registration errors are eliminated, and patient scanning time is reduced.** The random count rate rises from 5% in a routine FDG study to 20% during a simultaneous transmission scan. There is no significant difference in measured activity concentrations from independent and simultaneous emission scans over a 110:1 activity concentration, nor in regional attenuation coefficients measured pre and post isotope injection.

The technique is especially useful in FDG and F-DOPA studies where the long time between isotope injection and final imaging previously required immobilization following the pre-injection transmission scan until the end to the emission scan.

* Now at University Hospital, University of Pennsylvania

Neurology

Posterboard 1154

EVALUATION OF EARLY AND DELAYED SPECT WITH I-123 IODOAMPHETAMINE IN THE ASSESSMENT OF ACUTE BRAIN INJURY. H.J. DeBlanc, Jr., J.R. Mawk, M.C. Johnson, F.N. Hegge. Emanuel Hospital, Portland, OR.

Within 24 to 72 hours of acute cerebral trauma 75 patients received I-123 Iodoamphetamine (IMP) SPECT scans employing standard gamma camera techniques at 20 minutes and 4 hours after IV injection. All had serial CT scans, some had subsequent MR scans, and some had prior emergency neurosurgical stabilizing procedures.

IMP SPECT clearly demonstrated focal lesions in early and delayed scans that correlated closely with CT and MR results. Additional lesions were found in SPECT scans of some patients that were not present in CT scans. Four basic patterns of initial and delayed cerebral activity were observed and clinically interpreted as follows:

Initial (20 min)	Delayed (4 hrs)	Interpretation
Normal	Normal	No detectable lesion
Diminished	Normal or Improved	Cerebral ischemia, edema, elevated ICP
Normal	Diminished	Anoxia, preinfarction, luxury perfusion
Diminished	Diminished	Infarction

The correlation of the time/activity relationship in focal cerebral lesions on IMP SPECT scans with CT and MR results provides a new dimension in evaluating the clinical status of acute brain injury patients. IMP SPECT is useful prognostically, disclosing regions of contusion or ischemia missed by CT and MR, identifying superimposed brain insults (anoxia, elevated ICP, edema) and discriminating between infarction and edematous or potentially viable, though injured tissue.

Posterboard 1155

CYTOARCHITECTURAL PATTERN OF CEREBRAL BLOOD FLOW MEASURED BY SQ 32097. R.J. Di Rocco, B.L. Kuczynski, D. Silva, T. Feld, C. Ita, R.K. Narra, A.D. Nunn and W.C. Eckelman. The Squibb Institute for Medical Research, New Brunswick, NJ

SQ 32097, Chloro [bis [2,3-butanedionedioxime(1-)-O][2,3 butanedione dioximato (2-)- N,N',N",N"',N"",N""] (2-methylpropyl boron) technetium, is a member of the BATO family of neutral lipophilic technetium complexes. Herein, we report details of its cytoarchitectural distribution in monkey brain after intravenous administration. Gray level measurements of gray and white matter regions of transverse cynomologus monkey brain autoradiograms were obtained using computer assisted image analysis. The gray levels were converted to relative optical density (ROD) for determination of gray/white ratios. The gray/white ratios for cortical regions were 3.28 (frontal), 3.62 (parietal) and 4.39 (occipital) yielding a weighted average of 3.56 for the entire cortex at a 10 min residence time. At 60 min, the values were 1.53, 1.75 and 1.69, respectively, yielding a weighted average of 1.68. The change in value of the gray/white ratio between 10 and 60 minutes can be attributed to differential washout.

The distribution of acitvity within the cortex is heterogenous. In particular, a dark band of activity in occipital and somatosensory cortices appears to correspond to layer IV, which contains numerous axon terminals of thalamocortical projection fibers. The molecular layer of the hippocampal formation is another dense neuropil that is heavily labeled in these autoradiograms. Layer IV of the neocortex and the molecular layer of the hippocampal formation have high metabolic rates as measured by ^{14}C-deoxyglucose autoradiography. Therefore, the monkey brain images we have obtained using SQ 32097 correspond to the known cytoarchitectural pattern of cerebral glucose metabolism. In light of the tight coupling between flow and metabolism in the brain during normal physiological states, this finding satisfies a necessary condition for demonstrating that SQ 32097 measures cerebral blood flow.

Posterboard 1156

PET SCAN OF BRAIN GLUCOSE METABOLISM IN PSYCHIATRIC PATIENTS WITH SUMMER SEASONAL AFFECTIVE DISORDERS.
P.F. Goyer, P.M. Schulz, W.E. Semple, M. Gross, T.E. Nordahl, A.C. King, T.A. Wehr, R.M. Cohen, Brain Imaging Division, NIMH, Bethesda, MD.

The purpose of the study was to investigate potential differences in brain glucose metabolism between normal controls and summer seasonal affective disorders, SSAD.

5mCi of F-18-deoxyglucose were administered intravenously to each of nine psychiatric patients(mean age =49.9 years, SD = ± 11.3 years) who were diagnosed as SSAD according to previously published criteria of Wehr and Rosenthal. Patients were scanned in June through August using a Scanitronix PET scanner with a 5-6mm FWHM in plane resolution. On the day of the scan all patients had a Hamilton Depression Rating of greater than 14(mean = 18.5, SD = ±3.6). Two blinded raters used 5 standard planes to independently measure 60 regions of interest (ROI) as previously described by Cohen et al.

Nine age and sex matched controls underwent scan procedures identical to the SSAD patients.

Although absolute glucose metabolic rates, based on the Sokoloff method, were available for all subjects, comparison between groups was performed using ROI counts normalized by whole brain counts. Using a two tailed T test, 7 of the regions showed differences significant at $p < .05$ with four regions showing increased metabolism and three regions showing decreased metabolism. All seven of these regions, plus one additional, were confirmed with a larger non matched control group of 50 subjects.

To the authors knowledge, this is the first demonstration of in-vivo metabolic brain differences in patients with the controversial diagnosis of SSAD.

Posterboard 1157

TOMOGRAPHY OF Tc-99m-d,l-HMPAO OF BRAIN VOLUME AND ITS NEUROANATOMY.
T.J. Hoffman, G. Valle, R. Fuentes, A. Singh and R.A. Holmes. Nuclear Medicine and Research Services, Harry S. Truman Memorial Veterans Hospital, Columbia, MO.

For a better understanding of the brains' neuroanatomy using Tc-99m-HMPAO tomographic images, we superimposed anatomicaly labeled sections employing a photographic computer unit used to do quantitative autoradiography (Am. J. Phys. Imaging 3:81-90, 1988). SPECT brain images were produced from circumferential head counts of patients with suspected cerebrovascular disease using a Siemens ZLC 7500 rotating head camera, LEAP collimator and an ADAC 3300 computer. Twenty-five mCi of Tc-99m-d,l-HMPAO were used (>95% lipophilic chelate). A back-projection algorithm was used for image reconstruction. Tomographic slice thickness is 6.6mm and in-slice resolution is 1.2 cm. Total brain volume is displayed in 16 slices from 3 orthogonal views (sagittal, coronal, transverse). Four selected tomographic slices of each view were labeled and superimposed over the appropriate Tc-99m-HMPAO section. Structures such as the substantia nigra, the red nucleus, the caudate, putamen and pons can be accurately localized. Current results indicate that reasonable anatomic localization can be demonstrated with SPECT brain imaging.

Posterboard 1158

DISCORDANCE BETWEEN CONSECUTIVELY ACQUIRED "DUAL" I-123 ISOPROPYL-IODOAMPHETAMINE (IMP) AND TC-99M EXAMETAZIME (HM-PAO) SPECT BRAIN SCANS IN SUBACUTE CEREBRAL INFARCT.
J.S. Nagel, P.A. Carvalho, R.J. English, J.L. Moretti, J. Jarden, K.A. Johnson, R.E. Zimmerman, B.L. Holman. Brigham and Women's Hosp, Harvard Med School, Boston,MA.

I-123 IMP and Tc-99m HM-PAO are both used as cerebral perfusion imaging agents, but discrepancies have been noted in the relative uptake of these two radiotracers, particularly in subacute infarcts. To assess this phenomenon, pairs of IMP and HM-PAO scans were acquired for comparison using a rotating gamma camera equipped with a long-bore collimator. Without moving the patient sequential injection and imaging of 185 MBq IMP and 925 MBq HM-PAO were performed. The I-123 downscatter into the higher count Tc-99m images was minimal. "Dual" IMP/HM-PAO scans obtained on four patients after cerebrovascular accidents were analyzed visually as follows:

Patient No.	No. Days After CVA	Decreased Uptake IMP vs HM-PAO	Increased Uptake IMP vs HM-PAO
1.	11	Yes = Yes	Yes < Yes
1.(F/U scan)	55	Yes > Yes	
2.	14	Yes > ?	
3.	4	Yes > ?	
4.	4	No = No	

In general deficits were more prominent (>) with IMP than HM-PAO. Two scans had only minimal (?) abnormalities. Pt No.1 is notable for deficits plus a central area of increased uptake that was more prominent with HM-PAO than IMP and resolved on a follow-up scan. This finding may be due to breakdown of the blood brain barrier or luxury perfusion. These discordances reflect differing pharmacological properties of IMP and HM-PAO and are particularly important in subacute infarctions.

Posterboard 1159

CEREBRAL BLOOD FLOW : CORRELATIONS BETWEEN Xe-133 SPECT AND Tc-99m-HMPAO UPTAKE BY MEANS OF A DEDICATED BRAIN IMAGING DEVICE.
J Villanueva-Meyer, C Thomas, I Mena. Imaging Center, Harbor-UCLA Med Ctr, Torrance, CA.

The aim of this study is to explore the relationship of Tc-99m-HMPAO (HMPAO) uptake to regional cerebral blood flow (rCBF) by Xe-133 SPECT. 20 adults had Xe-133 rCBF SPECT and HMPAO SPECT scans within 2 hours. A dedicated brain scanner (Shimadzu, Set 031) was used. The resolution of the system for HMPAO SPECT is 8 mm at the cortex and for Xe-133 rCBF, 20 mm. One transaxial slice from the Xe-133 rCBF SPECT at the level of the basal ganglia was compared with the corresponding slice from a HMPAO SPECT. Cortical regions of interest were defined over each hemisphere in both SPECT studies. The Xe-133 rCBF values were correlated to counts per pixel from the HMPAO studies. Correlations were performed for the mean, highest and lowest values of rCBF.

Results show weak correlations over the entire range of rCBF (from < 20 to 100 ml/ 100gr /min) between HMPAO uptake and rCBF, r values range from .22 to .34. This observations suggest that the brain uptake of HMPAO is complex and that factors other than rCBF may be involved, (blood brain barrier characteristics, backdiffusion from the brain, HMPAO conversion between lipophilic and meso forms).

Both SPECT studies complement each other,. Xe-133 SPECT measures rCBF and HMPAO provides a high resolution image of relative brain uptake that indirectly relates to perfusion. Direct estimations of rCBF from HMPAO uptake are not warranted.

Posterboard 1160

PET IMAGING OF CENTRAL SEROTONIN RE-UPTAKE SITES IN THE BABOON BRAIN WITH [C-11]-N-Me-PAROXETINE (C-11-MPx). V.L. Villemagne, R.F. Dannals, P.M. Sánchez-Roa, U. Scheffel, H.T. Ravert, A.A. Wilson, T.K. Natarajan, J.J. Frost, H.N. Wagner Jr. The Johns Hopkins Medical Institutions. Baltimore, MD.

Central serotonin re-uptake sites are involved in depression, suicide, appetite control, thermoregulation and pain. An analog of the selective and potent inhibitor paroxetine, N-Me-paroxetine, was labeled with the positron emitter C-11. In the present study, we evaluated the distribution and kinetics of C-11-MPx binding to serotonin uptake sites using positron emission tomography (PET). After intravenous injection of 20 mCi of high specific activity C-11-MPx (2800 mCi/μmol) into a 35 kg anesthetized baboon (Papio Anubis), sequential quantitative tomographic slices, passing through the cerebellum (CB), hippocampus (HP), frontal (FR) and parietal (P) lobes, were obtained over a period of 90 min. Brain activity plateaued within 20-30 minutes post injection of the radioligand. Treatment with 1 mg/kg paroxetine i.v. five minutes prior to the injection of the radiotracer reduced the FR/CB, P/CB and HP/CB ratios from 1.35, 1.26 and 1.30 to 1.10, 1.01 and 1.16, respectively. The regional brain uptake and the degree of blockade at 90 min highly correlates (r=0.84 and 0.92 respectively) with the regional in vitro specific binding of [H-3]-imipramine to serotonin uptake sites in human autopsy brain: high in frontal and parietal lobes, intermediate in the hippocampus, and very low in the cerebellum. These results demonstrate the feasibility of in vivo imaging of serotonin re-uptake sites with PET and suggest that C-11-MPx can be used to evaluate these binding sites in the human brain in vivo. This method could be used to monitor antidepressant drug therapy; and in the study of the pathophysiology of psychiatric disorders such as depression and serotoninergic neurotoxicity.

Posterboard 1161

^{123}I IMP REGIONAL CEREBRAL BLOOD FLOW: QUANTITATIVE INDICES IN NORMAL SUBJECTS. D.A. Weber, P.S. Klieger, N.D. Volkow, D.F. Sacker, G-J Wang and M. Ivanovic. Brookhaven National Laboratory, Upton, NY.

Quantitative SPECT and planar imaging is used to investigate localization and clearance properties of intravenously administered ^{123}I-iodoamphetamine (^{123}I-IMP) in normal subjects. The study provides a quantitative data base of the imaging properties of ^{123}I-IMP uptake in the brain needed as a reference standard in the study of brain pathology. Eight subjects have completed two ^{123}I-IMP studies. Each study included dynamic imaging of ^{123}I-IMP uptake in the brain measured between 0-15 m post injection (p.i.); SPECT imaging of the brain at 30 m, 3 h and 4 h p.i.; and whole body scans at 75 m p.i. ^{123}I blood clearance was measured between 0 and 4 h.

Quantitative indices of cerebral perfusion calculated from ROIs placed over the cerebral cortex (CC), the cerebral vascular territories (CVTs) and functional areas of the brain revealed marked differences in regional ^{123}I uptake. Observations include reproducible clearance of ^{123}I-IMP from the brain in repeat SPECT studies (e.g. mean clearance from cerebellum of 24.4±4.1% in the first study vs 25.4±4.7% in the second study and from basal ganglia: 14.9±7.2%/14.8±3.7%) and reproducible contralateral uptake ratios in the CC on early SPECT images. Significant differences in metabolic clearance of ^{123}I-IMP observed between smokers and nonsmokers markedly decrease count levels seen in SPECT images(% retained dose at 1.5 h: brain 3.7±0.4%, lung 30.3±0.9% in smokers; brain 5.3±0.3%, lung 20.9±0.8% in nonsmokers).

Nuclear Magnetic Resonance

Posterboard 1162

IN VIVO VALIDATION OF NMR VELOCITY MEASUREMENTS IN SMALL ARTERIAL VESSELS. R.E. Wendt III, R. Rokey, W.-F. Wong, and A.G. Marks. St. Luke's Episcopal Hospital, The Methodist Hospital, and Baylor College of Medicine, Houston TX.

The patency of and nature of the flow in an artery is reflected in the distribution of blood flow velocities in the vessel. Currently, it is difficult to measure velocities in small, deep vessels noninvasively. This study tested the ability of NMR to measure velocities in the rabbit aorta.

Five male, New Zealand white rabbits weighing from 4 to 6 kg were examined. Each was sedated, anesthetized, intubated, and ventilated. An ultrasonic crystal for range-gated pulsed Doppler velocity measurements was placed directly on the descending aorta. The aortas ranged in circumference from 8 to 11 mm and had an average area of 1.68 mm^2.

Sixteen transaxial, velocity-compensated, gradient-refocussed echo, perpendicular-velocity-resolved, EKG triggered images were acquired using a 2.4T, 40 cm bore NMR imager. The "Nyquist velocity" of the pulse sequence was 90 cm/s. Velocity-resolved data were acquired immediately after the R-wave, at mid-systole, at the time of the peak of the Doppler velocity measurement, late in systole, and early in diastole.

The flow information from the velocity images was condensed into velocity spectra. A region of interest for the entire aorta, which typically was covered by only four pixels, was defined and a velocity spectrum or histogram was produced by summing the pixels in the region for each of the velocity images.

A linear regression of the peak velocities measured by the two techniques gives $V_{Doppler} = 0.752\,V_{NMR} - 6.30$ cm/s with an R value of 0.94. Velocity spectra constructed from the Doppler velocity profiles have the same shapes as the NMR velocity spectra. The measurements of peak velocity by NMR and Doppler ultrasound agree well.

Oncology/Hematology

Posterboard 1163

F-18 FDG UPTAKE IN BENIGN AND MALIGNANT MUSCULOSKELETAL TUMORS. L.P. Adler, H.F. Blair, J.T. Makley, M.J. Joyce, G.P. Leisure, G.J. Muswick, A.D. Nelson, F.D. Miraldi. University Hospitals of Cleveland and Case Western Reserve University, Cleveland, OH.

Previous research has shown a positive correlation between histological grade and the degree of FDG uptake in brain tumors. This data represents our initial experience comparing FDG uptake with PET scanning in patients with benign and malignant musculoskeletal tumors.

Nine patients with tumors of the musculoskeletal system received PET scans following the administration of between 3 and 11 mCi of FDG. The patients were divided into three groups. Group 1 consisted of four benign tumors (fibroma, pigmented villonodular synovitis, non-ossifying fibroma, and a ganglion synovial cyst). Group 2 patients consisted of three low grade malignancies (two liposarcomas and one angiosarcoma) while group 3 was composed of two patients with highly malignant lesions (a malignant fibrous histiocytoma and osteosarcoma). Tumor to background ratios and both average and peak tumor uptake of FDG (normalized by the dose administered and the patients weight) were then calculated for each tumor.

One way analysis of variance demonstrated significant differences between the three groups for each of the measures of FDG localization ($p = .01$ for ratios, .002 for average tumor uptake, and .005 for peak tumor uptake). There was significant correlation between histological grade and FDG uptake ($r = .75$ for ratios, .85 for average tumor uptake, and .88 for peak tumor uptake).

Posterboard 1164

PET EVALUATION OF REGIONAL CHEMOTHERAPY IN PATIENTS WITH LIVER METASTASES USING F-18-URACIL AND O-15 LABELED WATER. A. Dimitrakopoulou, L.G. Strauss, J.H. Clorius, P. Schlag, F. Helus, J. Doll. German Cancer Research Center, Heidelberg, Germany.

Fluorouracil (FU) has found use for both intravenous and intraarterial chemotherapy in patients with liver metastases from colorectal tumors. We used PET and F-18-uracil to compare the uptake of the cytostatic agent in metastases and normal liver parenchyma after intravenous and intraarterial tracer application. Furthermore, O-15 labeled water was administered to evaluate the perfusion pattern. The evaluation comprises 26 double examinations (intravenous and intraarterial studies) in 13 patients with surgically implanted catheters in the gastroduodenal artery. Standardized tracer concentrations (DAR values) were calculated using a ROI technique for the metastases, normal liver parenchyma and the aorta. The FU concentrations 2 hours after tracer application were higher in 10 of 18 metastases using the i.a. approach, while in 4 metastases the concentrations were lower following i.a. FU infusion. In one patient a five fold increase in FU uptake was noted after i.a. tracer application. We observed a higher systemic toxicity in 33 % of the patients. While the accumulation of the perfusion tracer O-15 labeled water was up to 10 times higher in the metastases after intraarterial injection, the FU uptake was not significantly increased by the regional application. Therefore, perfusion studies alone cannot be used to estimate the chemotherapy outcome. The results of the ongoing study demonstrate, that PET with F-18-uracil should find preferential use to optimize the regional chemotherapy and to select those patients who do profit from the intraarterial approach.

Posterboard 1165

POSITRON EMISSION TOMOGRAPHY (PET) WITH F-18-DEOXYGLUCOSE IN SMALL CELL CARCINOMA. M.V. Knopp, L.G. Strauss, A. Dimitrakopoulou, H. Manke, J. Blatter, F. Helus, G. van Kaick. German Cancer Research Center, Heidelberg, Germany.

Positron emission tomography (PET) with F-18-deoxyglucose (FDG) was used in patients with small cell carcinoma in order to determine the metabolism of the tumor prior and during chemotherapy. Furthermore, O-15 labeled water and N-13-glutamate were administered in selected cases to evaluate the tumor perfusion and metabolism. Tracer concentrations were obtained using a ROI-technique and standardized for the injected dose and the body volume. All patients had a CT scan shortly before the PET examination. The tumor volume was calculated from the CT-images using a three axis method. Thirty patients with histologically confirmed small cell carcinoma were included in the ongoing study. Follow up studies during chemotherapy were performed in eight patients for a maximum period of 167 days. All tumors showed a significant FDG uptake in comparison to the surrounding normal structures and were readily visualized on the PET cross sections. The standardized concentration values (DAR values) were in the range of 1.58-6.52 with a median value of 2.90. We noted a low correlation (r=0.511) in 10 patients between the FDG uptake prior to the first chemotherapeutic cycle and the survival. Three patients had positive mediastinal lymph nodes and a significant FDG accumulation, while N-13-glutamate had the highest lymph node uptake. The change in tracer concentrations showed to be a more sensitive parameter for therapy response than the change in tumor volume. These preliminary data demonstrate, that PET is a promising method for treatment monitoring of patients with small cell carcinoma.

Posterboard 1166

DISTRIBUTION AND CONCENTRATION OF L6 BINDING SITES BY IN VITRO QUANTITATIVE AUTORADIOGRAPHY. S. Lastoria, J.C. Reynolds, J.A. Carrasquillo, R.D. Neumann. Nucl. Med. Dept. N I H Bethesda, MD.

Mouse monoclonal antibody L6 (IgG2a) binds to a ganglioside antigen (GD) expressed by human breast, colon non-small cell lung and ovarian carcinomas.

We investigated the tissue distribution and molar concentration of GD in frozen sections from 12 non small cell lung cancer using in vitro quantitative autoradiography (QAR) method (J.C. Reynolds et al. JNM: 29s, 5, 1988, pp 897).

Chloramine-T method was used to label L6 IgG2a with I-125 (Sp. Act. 1.06 uCi/ug). The I-125 L6 immunoreactivity tested on H3357 colon cancer cell line, by cell binding assay, was 69%.

Autoradiographic images of tumors and I-125 standards were digitized by microdensitometry. Regional tissue radioactivity was measured, and by computer analysis the maximal specific binding (Bmax), and the affinity constant (Ka) were calculated.

The Bmax values ranged from 37 to 414 pmoles/g in 11 tumors; one tumor and normal lung had undetectable levels of GD. The pattern of GD distribution was homogeneous in 4 lesions and localized in well defined areas in 7 tumors.

The high GD antigen levels, measured by QAR, as well as L6 IgG2a immunological properties strongly support its use in radiolabeled antibody scintigraphy and therapy.

Posterboard 1167

THE EFFECT ON MARROW AND TUMOR OF BONE CANCER AGENT Sn-117mDTPA vs P-32. L.F. Mausner, R.F. Straub, G.E. Meinken, S.C. Srivastava, H.S. Burlington, E.P. Cronkite. Medical Department, Brookhaven National Laboratory, Upton NY

We have previously shown that Sn-117m(+4)DTPA has high bone tumor uptake and low soft tissue deposition in various animal models. The decay of Sn-117m (t1/2=13.6d) provides internal conversion electrons (129.4 and 151.6 keV at 64.8% and 26.1% respectively) with an imageable gamma ray (158.6 keV, 86.4%). Since the bone uptake is onto bone mineral surfaces, the short range of the monoenergetic electrons (0.3mm in water) should be less marrow damaging than high energy β emitters commonly used to treat bone metastases. To test this hypothesis, the effects on bone marrow of paired doses of Sn-117mDTPA and P-32 were compared using the Colony Forming Units per Spleen (CFU-S) Assay. Mice (CBA/Ca) were injected with Sn-117mDTPA or P-32 at three activity levels, which were calculated to deliver 180, 420 and 600 rads to bone at 4 days. The mean CFU-S per femur was measured to be 63%, 29%, and 18% of the control for Sn-117mDTPA and 29%, 4%, and 0.6% for P-32. These data clearly demonstrate the marrow sparing advantage of Sn-117mDTPA vs P-32, particularly at higher doses. A comparison of therapeutic efficacy of these two agents is now underway. Mice (C57B) with subcutaneously implanted osteosarcoma were injected with the same activity levels of Sn-117mDTPA or P-32 as previous, resulting in a total bone dose of 1000, 2333 and 3333 rads. Control animals were injected with cold SnDTPA or saline. The tumor growth relative to these controls is being monitored and will be described.

Pediatrics

Posterboard 1168

VALIDATION OF THE GATES GFR METHODOLOGY IN CHILDREN. LEONARD JC, BUROW DM, WENZL JE, PUFFINGBARGER WR. CHILDREN'S HOSPITAL OF OKLAHOMA AND THE UNIVERSITY OF OKLAHOMA SCHOOL OF MEDICINE, OKLAHOMA CITY.

The Gates method of measuring GFR is widely used to assess renal function in children, but the youngest patient in his series was 17y. Schwartz has published formulas which relate serum creatinine (SCr) to creatinine clearance based on the patient's height and an age specific constant. We identified 85 patients with a Gates GFR, using background regions inferior to the kidneys, who had a SCr determination within 24 hours and compared the resultant calculations of GFR.

AGE	7d≤age≤1y	1y<age<13y	13y - 22y
NUMBER	16	39	18
INTERCEPT	27.42	36.54	15.7
R VALUE	0.831	0.739	0.848

Testing of the mean differences failed to show any significant difference between the methods. With a lateral background there was no significant difference between the methods, but the two Gates methods are not identical when using the same regression equation. The inferiorly placed regions yield a consistently higher value. In addition, correcting for body surface area resulted in a grossly overestimated GFR for infants, with less effect being noted as the child approached a standard 1.73m2 surface area.

In conclusion, the Gates method is accurate for monitoring renal function in children, and is the preferred method whenever individual renal function must be assessed. In addition, the method intrinsically corrects for body surface area differences.

Posterboard 1169

COMPARISON BONE SCINTIGRAPHY AND MR FOR THE EVALUATION OF PATIENTS WITH AN EARLY STAGE OF LEGG-CALVE-PERTHES DISEASE. M. Oshima, K. Itoh, H. Fukatsu, H. Asai, and S. Sakuma. Nagoya University school of Medicine, Nagoya, Japan.

The aim of this study is to evaluate 18 patients with an early stage of Legg-Calve-Perthes disease using both bone scintigraphy and magnetic resonance(MR) imaging. The population studied included 16 males and 2 females(range 4-12 yr). Bone scintigraphy was evaluated with pinhole image(PIN), and MR was evaluated with T1-weighted(T1) and T2-weighted(T2) spin-echo. Both studies were performed within one month.

In an initial stage(n=5), x-ray showed an enlarged joint space without reduction of epiphyseal size, PIN showed a complete void in the femoral capital epiphysis in 3/5, while MR showed low density-zone(T1) in the same area. In the other 2/5 initial stage, PIN showed marked uptake in the capital with small defects. In these cases, MR showed deformity of femoral capital and cartilage(T1). In the sclerotic stage(dense epiphysis) (n=13), PIN showed a void in 4/13 with low-intensity zone(T1). In the other 9/13 sclerotic stage, PIN showed a void with lateral column correlated with low-intensity zone (T1) and high-intensity lateral(T2). Lateral column and high-intensity lateral will represent hyperemia or early revascularization. In summary, PIN was able to differentiate the necrotic area from hyperemia clearly than MR, while MR delineated articular cartilage and the shape of capital femoral epiphysis which were not visualized in PIN.

Pulmonary

Posterboard 1170

Back-flow Testing of CPR Airway Valves with Radioactive Gas,(^{133}Xenon).

K. Hairfield and M.J. Hagler, Kern Radiology and Nuclear Medicine Group and Bakersfield College, Bakersfield, California.

Several masks, face and mouth covers and one-way valve mechanisms are available on the market or are being currently developed for use in CPR. With public concern for the potential of communicable diseases, it is of importance to establish the competency of those devices to ensure continuing private and public participation in CPR.

The valves in five CPR devices were tested by placement of a reservoir of ^{133}Xe and room air on the output (victim) side of the device's one-way valve. Another reservoir with only room air was attached to the input (rescuer) side. A closed system resulted. Camera images and count rates were taken post-injection of .4 millicures of ^{133}Xenon at one, eight, and fifteen minutes at passive equilibration. A twenty minute interval was recorded for each device with the addition of positive, back-pressure.

Two out of the five valves tested demonstrated bi-directional flow. The valves tested were from the following devices: Brooks Life-Saving Airway, Laerdal Pocket Mask, Microshield, Puritan Manual Resuscitator, and "Kiss of Life" Mask.

Posterboard 1171

QUANTITATIVE COMPARISON OF V/Q AND CT FOR IDENTIFYING EMPHYSEMA IN ALPHA-1 ANTITRYSIN DEFICIENCY. T.R. Simon, G. McElvaney, I. Feuerstein, R. Hubbard, and R.G. Crystal. Departments of Nuclear Medicine and Radiology, and Pulmonary Branch, NHLBI, National Institutes of Health, Bethesda, MD.

Recent advances in treating alpha-1 antitrypsin deficiency (A1AT) now make timely identification of those patients developing emphysema clinically important. Since both ventilation/perfusion scintigraphy (V/Q) and CT purport to localize emphysema, we performed a quantitative comparison of these techniques using the diffusing capacity (DLCO) as a measure of current emphysema.

Regions in both lungs at the apical, carinal and basal levels were compared. V/Q used Xe-133 gas to establish lung boundaries and Tc-99m MAA to determine the percentage of perfusion in each region. Counts were normalized for region size and expressed as a percentage of total counts collected in all regions.CT quantitation was based on the direct observation method of Sakai et al [J.Comput.Assist.Tomogr.11:963-968, 1987] that provides a severity-extent product to describe the disease in regions equivalent to those used for V/Q analysis.

Of the 8 patients studied, 1 (13%) was normal by DLCO (125% predicted). In this patient, the V/Q was normal while the CT displayed only minimal disease. V/Q showed all the remaining 7 (88%), had abnormally low bilateral basal perfusion (13%±5%, mean±SD) characteristic of this disease. CT found predominantly basal disease in 6 of these 7 (86%).

Thus both V/Q and CT showed high sensitivity for diffusional compromise in A1AT. When abnormal, they demonstrated a similar distribution of disease in 6 of 7 cases.

Radiopharmaceutical Chemistry

Posterboard 1172

SYNTHESIS AND BIODISTRIBUTION OF TRITIATED CRYPTAND 2.2.2. K Garmestani, JM Link, KA Krohn, Dept of Radiology, Univ. of Washington, Seattle, WA.

We are investigating a macrobicyclic polyether, cryptand 2.2.2, as a ligand for generator produced radionuclides for use as a freely diffusible indicator of blood flow. In order to measure the biodistribution of cryptates of 2.2.2, it was necessary to radiolabel the ligand. We have synthesized tritiated cryptand 2.2.2 by the reaction sequence below. The tritiated diborane was prepared from tritiated $NaBT_4$ and BF_3 in quantitative yield. The octanol-water partition coefficient of the cryptand was 0.3 and initial biodistribution data in mice are consistent with a freely-diffusible tracer. We are continuing *in vitro* and *in vivo* studies of cryptand complexes.

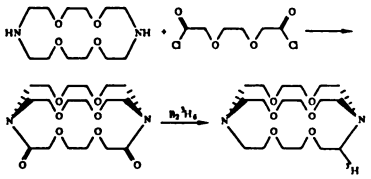

Biodistribution of cryptand 2.2.2 at 1 minute post injection in non-anesthetized mice

Tissue	%I.D./Organ	Tissue	%I.D./Organ
G.I.	20.1,21.3	Heart	1.5,0.7
Brain	0.35,0.32	Kidney	4.5,16.4
Liver	8.4,8.8	Muscle	4.3
Lung	4.4,1.4		

Posterboard 1173

[IODINE-124]2-IODOISONICOTINIC ACID HYDRAZIDE: A POTENTIAL RADIOTRACER FOR TUBERCULOMA. C.W. Somawardhana and R.M. Lambrecht, King Faisal Specialist Hospital and Research Centre, Riyadh, Kingdom of Saudi Arabia

Isonicotinic acid hydrazide (INH) has been one of the most effective agents in tuberculosis therapy since 1952. We have labelled the aromatic nucleus of INH with I-124 to be used as a possible radiotracer for differential diagnosis of tuberculoma. 2-Iodoisonicotinic acid (~1mg) was suspended in water (200 µl) and 5N sodium hydroxide solution (5 µl) and high specific activity sodium iodide -124 (100 µl) were added. The vial was capped tightly, and heated at 140°C for 2h. Then the solution was acidified with dilute hydrochloric acid until a faint precipitate appeared. The solvents were removed with the aid of a stream of nitrogen and the resultant material was extracted with methanol (3x500 µl). The methanol solution was treated with diazomethane until a persistent yellow color appeared. The solvents were evaporated and the residue was dissolved in ethanol (100 µl) and heated to boil. Then hydrazine hydrate (20 µl) was added and vortexed well. After 1 min the reaction mixture was analyzed by HPLC using carbon-18 reverse phase column, with acetonitrile: water (40v:60v) as the eluent. Retention times of free iodide, 2-iodomethylisonicotinate and 2-iodoisonicotinic acid hydrazide were 2.3, 12.3, and 3.0 min respectively. Overall radiochemical yield was (16±4)%. The time spent for chemical manipulations was 3.5 hours. I-124 is a unique radionuclide for diagnostic (PET) and therapeutic radiopharmaceuticals.

Posterboard 1174

AN EVALUATION OF Cu-64 PYRUVALDEHYDE BIS (METHYLTHIO-SEMI-CARBAZONE) (PTSM) FOR THE MEASUREMENT OF TISSUE PERFUSION. J.W. Babich, S.R. Cherry, P. Carnochan, J.McGuire, H. Sharma*. Institute of Cancer Research, Sutton and University of Manchester*, Manchester, U.K.

CuPTSM has been proposed as a potential blood flow tracer in the heart and brain (Green et al J Nucl Med 1988;29:1549). Labeled with generator produced Cu-62 ($t_{½}$=9.8min) this agent could enable repeat perfusion studies in PET centres without an on-site cyclotron. The aims of this study were to compare the distribution of CuPTSM with Co-57 labeled microspheres in the rabbit brain, and with Rb-86 in a rabbit tumor model (VX2).

Cu-64-PTSM was prepared by the addition of free ligand to an ethanolic solution of Cu-64-acetate. RCP was determined by silica gel/ethyl acetate TLC and was always >95%. Preliminary biodistribution data in rats showed good heart (2.3%) and brain (2.2%) uptake with prolonged retention. For normal rabbit studies (n=6) CuPTSM (4MBq) was injected i.v. followed at 45s by an intraventricular injection of 10^6 microspheres (15µm). The animals were sacrificed at 15min post admin. In tumor bearing animals CuPTSM (4MBq) was injected i.v. followed by Rb-86-Cl (2MBq) i.v. at 13min and sacrifice at 15min. Tissue samples were taken and %dose/g and %dose/organ determined.

Our results show a clear relationship between CuPTSM and microsphere distribution in the brain. The data best fit a 2nd order polynomial indicating a drop in extraction of CuPTSM at high flows (r=0.93). In the lower flow tumor tissue, CuPTSM and Rb demonstrate a linear relationship (r=0.98). This data indicates that CuPTSM may be useful in the measurement of tissue perfusion in the brain and in certain tumours using PET.

Posterboard 1175

DEVELOPMENT OF A METHOD FOR THE RADIOSYNTHESIS OF 6-[C-11]-D-GLUCOSE. JR Grierson, JE Biskupiak, JM Link and KA Krohn, Dept. of Radiology, Univ. of Washington, Seattle, WA.

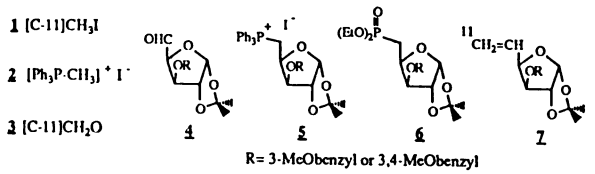

R= 3-MeObenzyl or 3,4-MeObenzyl

Synthetic methods for a practical radiosynthesis of 6-[C-11]-D-glucose from either labeled methyl iodide or formaldehyde are being evaluated. Studies involving unlabeled materials have indicated that an approach involving the use of phosphonium ylids (derived from 2 or 5) could be useful for the introduction of the label at C-6 in glucose. The speed and efficiency of several of the reactions on route to glucose have been examined. Of special note are: the conversion of methyl iodide to the ylid derived from (2) requires under 10 min.; the reaction of the ylide with the aldehyde precursor (4) requires under 30 min: the vic-hydroxylation of the resultant alkene (7) by the method of Sharpless (ref 1) requires 5-10 min and results in a favorable ratio (4.6-3.3:1) of D-glucose to L-idose analogs (protected sugars), regardless of which asymmetric catalyst is used. The unwanted idose analog can be completely removed from the mixture at this stage by HPLC and the deprotection of C-3 of the glucose can be accomplished in under 10 min with DDQ (ref 2). Conversion of labeled methyl iodide (1) to the alkene (7) has been carried out with a 15% radiochemical yield (EOB). Efforts to improve these processes and the alternate use of the phosphonate compound (6) are ongoing.

(1) Jacobsen EN, et al., J Am Chem Soc. 110, 1968 (1988); (2) Oikawa Y, Yoshioka T, Yonemitsu O. Tet Lett., 23, 885 (1982).

Posterboard 1176

NO-CARRIER-ADDED F-18-FOR-NO_2 AROMATIC NUCLEOPHILIC SUBSTITUTION REACTIONS OF NITROCINNAMIC ACID DERIVATIVES.
D.-R. Hwang, S.M. Moerlein, M.J. Welch. Mallinckrodt Institute of Radiology, Washington University School of Medicine, St. Louis, MO.

F-18-for-NO_2 nucleophilic substitution reactions of activated nitroarenes (NO_2-Ar-G, G = (o,p)-NO_2,CN,COR) are commonly used in the synthesis of F-18-labeled radiopharmaceuticals. In pursuit of a new synthesis of F-18-fluorodopa, we have investigated substitution reactions using o-nitrocinnamic acid derivatives, i.e. G = CHCHCOR. After 5 min of microwave treatment the radiochemical yields (RCY) of 2a,b were moderate (25%, 2b) to good (>40%, 2a). The reaction has been successfully applied to the synthesis of an amide derivative of GBR-12783, 2c, a dopamine uptake inhibitor, with a RCY of 10%. Under similar reaction conditions the reaction has failed to yield F-18-fluorodopa precursors 2d,e due to the decomposition of the nitrosubstrates, 1d,e. This reaction can be used as a general method in labeling amines with F-18-phenylpropyl group, either via the reduction of the F-18-cinnamic amide or via F-18-phenylpropyl halide prepared from 2a.

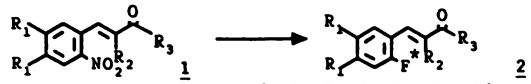

1 2

a: R_1-R_2-H, R_3-OEt b: R_1-R_2-H, R_3-piperidine
c: R_1-R_2-H, R_3-N⟨⟩N$(CH_2)_2OCH(Ph)_2$
d: R_1,R_1-OCH_2O, R_2,R_3- N=C(Ph)-O
e: R_1,R_1-OCH_2O, R_2-NHCOPh, R_3-OEt

Posterboard 1177

(S)-N-[(1-ETHYL-2-PYRROLIDINYL)METHYL]-5-(2[F-18]FLUOROETHYL)-2-METHOXYBENZAMIDE. A NEW PET RADIOTRACER FOR DOPAMINE D2 RECEPTORS.
J. Mukherjee, The University of Chicago, Chicago, Il.

A new [F-18]fluoride labeled dopamine D2 receptor radioligand has been synthesized for use in imaging postsynaptic dopamine D2 neuroreceptors by PET. The radiotracer, (S)-N-[(1-ethyl-2-pyrrolidinyl)methyl]-5-(2[F- 18]fluoroethyl)-2-methoxybenzamide (1) is an analog of sulpiride (the sulfonamide moiety in sulpiride. replaced with a fluoroethyl group), the clinically used antipsychotic drug belonging to the class of substituted benzamides. The precursor to this radiotracer, (S)-N-[(1-ethyl-2-pyrrolidynyl)methyl]-5-(2-toluenesulfonyloxyethyl)-2-methoxybenzamide was synthesized by first protecting 4-methoxyphenethyl alcohol as the tetrahydropyranyl ether in >95% yield. This ether was treated with n-butyllithium (-40°C) and CO_2 to give 2-methoxy-5-(2-tetrahydropyranyloxyethyl)benzoic acid in 30-40% yield. This substituted benzoic acid was then coupled with (S)-2(aminomethyl)-1-ethylpyrrolidine using dicyclohexylcarbodiimide at 0-5°C to give (S)-N-[(1-ethyl-2-pyrrolidinyl)methyl]-5-(2-tetrahydropyranyloxyethyl)-2-methoxybenzamide in 60-70% yield. Deprotection of the tetrahydropyranyl ether (oxalic acid, acetone-water, pH 3) gave the corresponding alcohol (>90%) which was then tosylated (toluenesulfonyl chloride, pyridine) to provide the tosylate precursor in 80-90% yield.

The tosylate precursor was reacted with [F-18]fluoride (solubilized with kryptofix and potassium carbonate) in acetonitrile at 90-95°C for 30 minutes. The radiotracer (1) separated by HPLC on a C_{18} column was obtained in 20-30% radiochemical yield in specific activities of 600-800 Ci/mM.

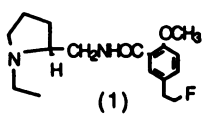

(1)

Posterboard 1178

THE PHARMACOKINETICS OF F-18-L-6-FLUORODOPA (FD) TRACER.
B.D. Pate, W.R.W. Martin, T.J. Ruth, M.J. Adam, K.A. Hewitt, and D.B. Calne. University of British Columbia and TRIUMF, Vancouver, B.C.

FD labelled with 2-hour F-18[1] is the tracer of choice for presynaptic function of dopaminergic neurons. This work was undertaken to explore in detail the neurochemical processes important in the uptake of the tracer into the striata and other areas seen in PET images. Cynomolgus monkeys (macacus fascicularis) were employed together with the UBC/TRIUMF PETT VI tomograph (in-plane spatial resolution about 9mm FWHM). Inhibitors for various enzymes and storage processes were administered to the subjects, a suitable time before fluorodopa PET scanning. Among the inhibitors used were: NSD 1015 (for AAAD); deprenyl (for MAO-B); and reserpine (for vesicular storage).

The two most important processes in striatal FD uptake are fluorodopamine vesicular storage (necessary but not sufficient) and FD decarboxylation (essential). Application of NSD 1015 one hour before the scan at 100 mg/kg reduced the striatal fluorodopa uptake constant[2] to 30% of normal. Application of reserpine produced a dose dependent reduction of striatal image intensity, the uptake constant reaching 30% of normal at 14 mg/kg. Application of deprenyl alone was not effective in reversing this reduction. F-18-3-O-Methyl-6-fluorodopa was employed to study the distribution of background activity in these scans, in comparison with that observed after NSD 1015 administration.

1)W.R.W. Martin et al. J. Nucl. Med. 27:6;1003(1986).
2)W.R.W. Martin et al. J. Cereb. Blood Flow and Metabol. 5:5593-5594(1985).

Posterboard 1179

FACILE SYNTHESIS OF CARBON-11 LABELED CITALOPRAM FOR P.E.T. STUDIES OF SEROTONIN UPTAKE SITES.
Siya Ram, K.R.R. Krishnan, G. Bissette, D. L. Knight, R. E. Coleman. P.E.T. Facility, Duke University Medical Center, Durham, NC 27710.

Citalopram [1-(3-(dimethylamino) propyl-1-(p-fluorophenyl)-5-phthalancarbonitrile, Lu 10-171] is a high affinity (Ki=0.7nM) selective serotonin uptake inhibitor used as an antidepressant. We have investigated an alkylation approach in the preparation of this compound as a P.E.T. ligand for the study of serotonin uptake sites which is of interest for various psychiatric disorders. Reaction of (C-11)CH_3I with desmethylcitalopram in acetone in the presence of sodium hydroxide base at 65°C for 8-10 minutes afforded [C-11] labeled citalopram which was characterized by TLC and HPLC in comparison with authentic cold sample of citalopram. Final purification over a silica gel Sep-pak cartridge using $CHCl_3$:CH_3OH:28% NH_4OH(5:0.9:0.1) gave pure [C-11] citalopram in 38% to 66% radiochemical yield (EOB) with radiochemical purity >95% for the exploratory C-11 synthesis. The time required for the manual synthesis and purification is 42-45 minutes from E.O.B. The specific activity of [C-11] citalopram was found to be 264 Ci/mmol [EOB]. Initial biodistribution studies in rats with (C-11) citalopram showed higher uptake in frontal cortex, substantia nigra and hypothalamus and further studies with this ligand are in progress.

Posterboard 1180

ROUTINE PRODUCTION OF [F-18]FLUORODEOXYGLUCOSE BY DIRECT NUCLEOPHILIC EXCHANGE ON A QUATERNARY AMMONIUM RESIN. S.A. Toorongian, D.M. Jewett, G.K. Mulholland, M.R. Kilbourn, M.A. Bachelor. Division of Nuclear Medicine, University of Michigan, Ann Arbor, MI.

In a simplified synthesis of [F-18]FDG, the radiolabeled precursor, [F-18]tetraacetyl-2-fluoro-mannopyranose, was obtained by direct nucleophilic substitution of the corresponding triflate with [F-18]fluoride trapped on a quaternary ammonium resin in a small column. The resin was a 2% crosslinked Merrifield resin quaternized with N-(4'-pyridinyl)-4-methylpiperidine, in the carbonate form. This resin was mixed with 20% by weight of a fibrous cation exchange resin in the H^+ form to improve liquid flow through the bed. A teflon column containing the resin (15 mg; 1.5 mm I.D. x 45 mm) was dried thoroughly and clamped in an aluminum heating block within an ionization chamber. [O-18]water from a silver target was passed directly through the column to extract the [F-18]fluoride. The resin was dried by 2 ml acetonitrile while the temperature of the column was raised to 100°. Then 1 ml of acetonitrile containing 20 mg of the precursor triflate was passed slowly through the column. The exchange reaction was monitored by the loss of radioactivity from the ionization chamber. The acetonitrile was evaporated, and the radiolabeled product was deacetylated by heating with 1 N HCl. In a series of 18 syntheses an average of 80 mCi (range: 19 mCi to 160 mCi) of [F-18]FDG was obtained for a target irradiation time of 15 min (p^+, 20 μA). Trapping efficiency for [F-18]fluoride ranged from 21 to 99% (average: 58%). Synthesis time was 40 min. Decay-corrected radiochemical yields ranged from 57% to 93%.

Posterboard 1181

HEXADENTATE BIFUNCTIONAL CHELATING AGENT: APPLICATION FOR RADIOLABELING OF ANTIBODIES. K.K. Bhargava, S. Chun and Z. Zhang. Albert Einstein College of Medicine, Bronx, N.Y.

Monoclonal antibodies labeled with metallic radionuclide can be used as molecular trucks to deliver tracer to tumors for noninvasive imaging. A hexadentate bifunctional derivative of the chelating agent triethylene tetra aminohexaacetic acid in which a isothiocyanatobenzyl moiety is attached to link this moiety to proteins was synthesized. The design of synthesis includes the reduction of 4-nitro-phenylalanylglycylglycine amide to relevant amine followed by carboxymethylation, reduction of the nitro group and resulted amino group to thiocyanato by thiophosgene (SCN-Bz-TTHA).

In-111 and Tc-99m labeling with this derivative was successfully achieved. The complex in each case yielded a single and stable entity in vitro and in vivo as confirmed by HPLC and biodistribution in mice. In-111 complex was also challenged by transferrin for 4 hours, there was no transfer of activity from In-111 complex to protein.

Conjugation of SCN-Bz-TTHA to human serum albumin (HSA) is effected by incubating the reactants (3:1 mole ratio) for 45 min at room temperature followed by purification of the HSA by dialysis at 5°C. When purified HSA was labeled with In-111, the labeling efficiency was found to be greater than 90% as shown by HPLC. Organ distribution in mice for the labeled preparation when compared with commercial RISA shows identical biodistribution.

Further work based on these results for labeling of antibodies by conjugating this bifunctional chelating agent is in progress

Posterboard 1182

AN AUTORADIOGRAPHIC STUDY DEMONSTRATING DIFFERENTIAL INTRATUMOR LOCALIZATION OF TWO MONOCLONAL ANTIBODIES IN NUDE MICE BEARING TRANSPLANTABLE HUMAN TUMORS. Chen EM, Li Z, Epstein AL, Taylor CR.

Previously we showed that a radiolabelled monoclonal antibody (TNT-1), directed against nuclear histones, can be used for imaging of different types of cancer in a nude mouse model (Cancer Res. 48:5842, 1988). A second monoclonal antibody (Lym-1), having specificity for B lymphocytes, was likewise shown to give imaging of a transplantable lymphoma (Raji). Autoradiography was utilized to explore the pattern of penetration of these two antibodies in the target tumors. Radioiodinated (I-125) TNT-1 or Lym-1 was injected intravenously into nude mice bearing either the ME180 human cervical carcinoma or the Raji lymphoma. Following injection, animals were sacrificed at intervals from 1 hour to 7 days. Tissue sections were developed for autoradiography, stained with H&E, and examined microscopically for the presence of granular deposits of silver that marked the microanatomic distribution of the labelled antibodies. In tumors biopsied at 1 hour post injection, the majority of the label was confined within blood vessels. From 2 to 6 hours, diffusion into the perivascular extracellular fluid was observed for both antibodies. Thereafter the patterns of distribution of Lym-1 in the Raji lymphoma and TNT-1 in the ME180 tumor progressively diverged. Lym-1 showed increasing concentration in a perivascular distribution, particularly at the tumor periphery. By contrast TNT-1 lost its perivascular distribution and instead demonstrated progressive concentration in the center of the tumor. The distribution patterns appear to reflect differences in site of first encounter of antibody with antigen. With Lym-1 the antigen is present on the surface of the tumor cells and is encountered immediately upon leakage of Lym-1 antibody from the microvasculature. Hence, Lym-1 accumulates perivascularly, or at the tumor periphery where permeability is marked. With TNT the antigen is intranuclear and is only accessible to antibody in areas where tumor cells show degeneration, rendering the cell membranes permeable to entry of antibody. Such areas tend to be deep within the tumor, and distant from blood vessels. These studies confirm the ability of TNT to bind areas deep within tumor that traditionally are considered inaccessible to antibodies administered for imaging/therapy.

Posterboard 1183

DEGRADATION OF TC-99m PERTECHNETATE IN SYRINGES WITH ALUMINUM-HUBBED NEEDLES. Hammes RJ and Schmidt MA, University of Wisconsin and William S. Middleton Veterans' Hospitals, Madison, WI.

During routine daily quality control via ITLC chromatography with acetone, a change in the radiochemical purity of 99mTc pertechnetate was noticed coincident with a change in brand of needle used, from a plastic-hubbed to plastic with an aluminum crimp at the hub (aluminum-hubbed) needles. Chromatography was performed on samples of freshly eluted TcO4 from 3 different generators using both types of needles fitted to identical syringes and spotted at various times from 0 to 60 minutes after drawing. pH was checked using narrow range paper. One set of samples was analyzed using a second solvent, normal saline. The results were expressed as the average percentage of total counts in the peak at the solvent front, (TcO4). The value for the aluminum-hubbed needles was 64.4% (n=24, S.D= 35.6), while that for the plastic-hubbed needles was 99.7% (n=11, S.D.=0.66). The appearance of impurities at the origin for the aluminum-hubbed needles was a function of time with the steepest slope at 20 - 30 minutes after drawing. Furthermore, a decrease in apparent concentration in the aluminum-hubbed needles was evidenced by a 78 % decrease in total counts on those chromatography strips relative to the plastic-hubbed needles' chromatograms, even though the spots used were the same size. The pH of the Aluminum-hubbed samples was 6.8 vs 6.2 for the plastic-hubbed samples. The behavior in saline solvent system was the same as in acetone. These results suggest that degradation occurs in the needles which have an aluminum crimp in the hub, leading toward an insoluble species of 99mTc. These insoluble impurities could lead to suboptimal images due to uptake in the reticuloendothelial system. This phenomenon was not observed with other Tc radiopharmaceuticals tested.

Posterboard 1184

VARIATION IN LABELLING EFFICIENCY OF THE ANTI-MELANOMA (NRX118.07.03) MOAB USING DIFFERENT 99m-Tc- GENERATORS. A.V. Heal, M. Courey, R. Schnieders, I. Tyson, and L. Tenorio. USF/Tampa VA, Tampa, FL.

At present, we are engaged in Phase III-Physician IND study for the clinical assessment of melanoma patients with 99m-Tc anti-melanoma MoAb (NRX118.07.03) for the diagnosis of melanoma and metastatic involvement. In order to perform this procedure the antibody is labelled with 99m-Tc by a ligand ester in a five step "in vitro" procedure with all material supplied by the sponsoring company. In the performance of this labelling procedure at different clinical sites, it was noted that there was a significant difference in labelling efficiency between a dry or wet 99m-Tc generator. The purpose of this study is to determine the cause of this difference.

Over fifty labelling procedures have been performed at the present time divided equally between the dry and wet generator. The labelling efficiency for each generator has been compared with the number of elutions, molybdenum break through, oxygen content and molecular form by TLC at each step in the procedure.

At the present time, the results indicate a slight correlation with oxygen content affecting the reduction of Tc for labelling and molybdenum break through with less pO-2, less molybdenum and better labelling efficiency for the wet generator. These results are not conclusive at the present time; however, studies are continuing in this area.

Renal/Electrolyte/Hypertension

Posterboard 1185

THE EFFECT OF CAPTOPRIL ON THE GLUCOHEPTONATE (GHA) SCINTIRENOGRAM IN RENAL ARTERY STENOSIS. B. Gale, C.G. Zhang, H.B. Lee, S. Heller, M.D. Blaufox, Albert Einstein College of Medicine, Bronx, N.Y.

A paradoxical increased GHA uptake is noted in kidneys excised and counted 3-5 min. after glucoheptonate (GHA) administration to awake rats with 2 kidney 1 clamp (2K1C) hypertension which received I.V. captopril 5 min. previous to GHA.This occurs more often ($P<0.01$) in rats with clamped kidney ERPF >0.6 ml/min/100g than in rats with clamped kidney ERPF <0.6 ml/min/100g. To test this observation in vivo, I-123 hippuran scans were obtained in anesthetized rats, followed by a control GHA scintirenogram (GHA I). After the control scan, captopril (1.3-1.7 mg/100g bwt.) was given I.V. and 5-10 minutes later a repeat GHA scintirenogram was obtained (GHA II).The rat was then killed, and the kidneys were weighed and counted.Scintirenograms were analyzed by drawing kidney and background regions of interest to produce time/activity histograms.Left renal activity (clamped kidney) was expressed as percent of bilateral renal activity.In 4/9 of the 2K1C rats the GHA I ratio from 3 to 5 minutes was greater than 50%. In the GHA II scan, none of the rats' GHA uptake from 3 to 5 minutes was over 50%.

This study does not confirm the previous observation of an increased early uptake of GHA in rats with RAS and mild reduction in function after captopril.However the previous study was done on awake animals.It is probable that the pentobarbital anesthesia in the post captopril scan caused sufficient reduction in renal function to prevent a similar finding.It is noteworthy that 4/9 animals had greater than 50% uptake of GHA on the stenotic side (mean uptake = 55%) prior to captopril. The hippuran uptake ratio in these animals was 41%.

Posterboard 1186

HIGH RESOLUTION TC99m-DMSA SPECT RENAL IMAGING, K. Levin, JW. Keyes, H. Ziessman, B. Harkness, Georgetown University Hospital, Washington, D.C.

Improved spatial and contrast resolution available on state of the art single photon emission computed tomographic (SPECT) gamma cameras should allow improved detection of focal defects in the renal cortex. We are performing SPECT renal examinations with Tc-99m-Dimercaptosuccinic acid (DMSA). A three detector SPECT system is used for image acquisition. The patients ranged in age from 4 months to 18 years old. Three-view pinhole and SPECT images were obtained in all patients. Review of the studies of ten patients (twenty kidneys) showed six kidneys that were normal on both studies; two kidneys that had possible focal cortical defects (FCD) on pinhole images had definite FCD with SPECT, seven kidneys that were normal with pinhole images had FCD with SPECT; three kidneys that were abnormal with pinhole images demonstrated additional FCD with SPECT; and two kidneys that were abnormal with pinhole images exhibited no additional FCD with SPECT. Generalized cortical thinning was demonstrated in eight kidneys by SPECT and not by pinhole images.

We feel that high resolution SPECT TC-99m-DMSA renal imaging improves the ability to identify focal renal cortical defects and to visualize asymmetry of cortical thickness.